MODELING AND CONTROL OF A GASOLINE DIRECT INJECTION FUEL SYSTEM

By

Mengyan Gu

A THESIS

Submitted to
Michigan State University
in partial fulfillment of the requirements
for the degree of

Mechanical Engineering – Master of Science

2015

ABSTRACT

MODELING AND CONTROL OF A GASOLINE DIRECT INJECTION FUEL SYSTEM

By

Menyan Gu

Fuel economy and emissions are the two main concerns to many automobile engineers. The Gasoline Direct Injection (GDI) fuel systems are widely used in internal combustion engines to improve fuel economy with reduced emissions.

This study focuses on the development of a MotoTron based fuel rail pressure control system. This work is motivated by the need for maintaining higher fuel rail pressure for improved fuel injection accuracy. The developed fuel rail control system consists of a MotoTron control module, a customized actuator drive box, and a host computer with LabVIEW GUI (graphic user interface) and the MotoTune calibration tool for MotoTron. The MotoTron and the host computer communicate through CAN (control area network). A mathematical model of the fuel rail control system was developed using MATLAB/Simulink.

The pressure controller for the fuel system contains three parts: a bumpless and anti-windup PI (proportional and integral) controller, a feed-forward controller, and a dead-zone compensator. The closed-loop control was simulated and validated in Simulink using the developed model, where the fuel injection process was also considered. The simulation results of tracking the desired pressure were compared with the experiment data.

The comparison with the Simulink simulation results and experiment data shows that the Simulink model is able to reflect the characteristics of the actual fuel rail system; and the experiment data show that the closed-loop controller is able to maintain the fuel system pressure at the desired level.

ACKNOWLEDGEMENTS

I would like to take this opportunity to express my sincere appreciation to many individuals who have so graciously helped me during my MS study. I would like to thank Dr. Guoming (George) Zhu for being my advisor and supporting me during my MS program and Dr. Harold Schock and Dr. Jongeun Choi for serving as advisors in my MS committee. And I would also like to thank Tom Stuecken and Kevin Moran for helping me set up the test bench and conducting the experiments. I would also like to thank students in our research group: Jie Yang, Tao Zeng, Yifan Men, Ruitao Song, and Ali M. H. Alhajjar who helped me to complete the MS research project.

Lastly, I am overly grateful for my parents' continued support and warm hearted solicitude that makes me full of courage to strive for the future.

TABLE OF CONTENTS

LIST OF TABLES

LIST OF FIGURES

KEY TO SYMBOLS AND ABBREVIATIONS

θ   Angle

Cos   Cosine

Kg   Kilogram

mm   Millimeter

mA   Milliampere

ρ Density (kg/m^3)

A   Section (m^3)

h   Piston displacement (m)

K_f Bulk modulus of elasticity

P   Pressure (bar)

q   Fuel flow (m^3/s)

u   Control signal

R   Resistance (Ω)

U   Voltage (V)

BDC   Bottom dead center

CAN   Controller area network

ECU   Engine control unit

ECM   Electronic control module

GDI   Gasoline direct injection

GUI   Graphic user interface

MRAC   Model reference adaptive control

MSU   Michigan State University

PFI   Port Fuel Injection

PI   Proportional and integral

RPM   Rotations per minute

TDC   Top dead center

CHAPTER 1: INTRODUCTION

1.1 Motivation

As an important key technology for improving the fuel economy of gasoline engines with reduced emissions, Gasoline Direct Injection (GDI) engines attract a lot of attentions. Compared with traditional Port Fuel Injection (PFI) engines, shown in Figure 1, GDI engines improve combustion efficiency with higher power density.
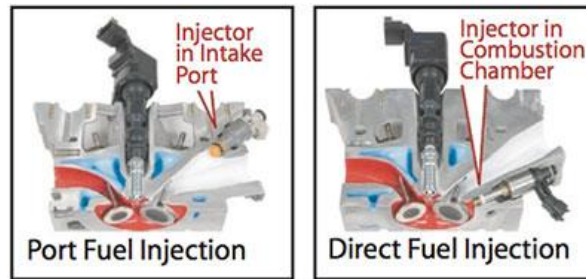
Figure 1: PFI Engine and GDI Engine

Improved fuel economy is mainly achieved by reducing throttling and heat losses during stratified combustion as well as operating the GDI engines with higher compression ratios than PFI engines. Furthermore, with the GDI concept, PFI wall-wetting and carbon buildup are eliminated inside the intake ports [1]. For the GDI fuel system, the gasoline is highly pressurized in the common fuel rail and injected via a GDI fuel injector directly into the individual combustion chamber. By injecting fuel directly into the combustion chamber, the charge mixing process during the intake stroke can be precisely controlled and optimized [2].

The fuel pressure for the fuel rail has fairly high pressure for GDI engines, and the fuel rail pressure fluctuations could affect fuel injection quantity accuracy and degrade the engine performance and even damage the engine. Therefore, the GDI engine fuel rail system needs to be precisely controlled, which is one of the key challenges for the gasoline direct injection technology. The main purpose of the fuel rail control is to maintain the desired fuel rail pressure

under all engine operational conditions, including fuel injection events, and make the pressure fluctuations as small as possible.

In this thesis, a GDI fuel rail pressure control system was developed using PI (proportional and integral) control and feed-forward control to minimize the fuel pressure fluctuation.

1.2 Existing Work

A number of studies have been conducted for the modeling and control of fuel rail systems and most of these studies are targeted at diesel engines. For example, the fuel rail system in reference [3] is developed based on the energy conservation principle; a physics-based mathematical model of the common rail system is developed in reference [4]; and a detailed fuel injection system simulation model for diesel engines is presented in reference [5].

Although the common fuel rail system for a diesel engine has a similar structure to the GDI fuel system, the fuel pump and the injector are quite different due to quite different fuel injection pressure. Therefore, modeling and control of the GDI fuel rail system is very different from the diesel fuel system. From a control point of view, back-stepping control strategy is used for the fuel rail system of a GDI engine in reference [6] and the Model Reference Adaptive Control (MRAC) algorithm is used to reduce the residual pressure in the fuel rail in reference [7]. This thesis intends to develop a control-oriented fuel rail model and validate it using the experiment data, and the developed model will be used for developing and validating the associated control algorithm.

1.3 Gasoline Direct Injection Fuel System Overview

1.3.1 System Block Diagram

In this research, the fuel rail system includes a fuel tank with a low pressure pump, a high fuel pressure pump driven by an electrical motor, a fuel rail, an injector, and a pressure relief valve. The GDI fuel rail system is able to pressurize the fuel rail up to 250 bar. The fuel rail pressure is independent of the engine speed; see Figure 2 for the system block diagram.
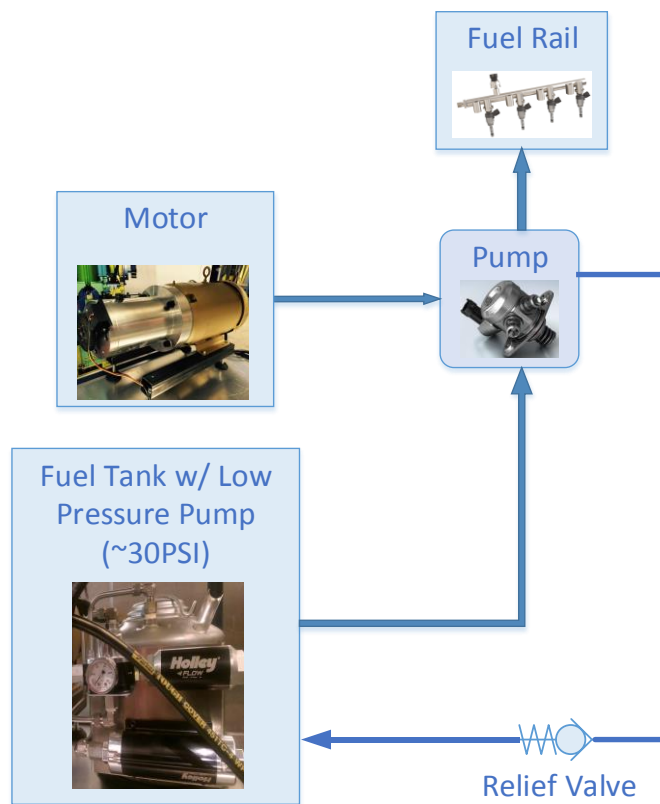
Figure 2: Fuel Rail System Block Diagram

The low pressure pump in the fuel tank increases the supply pressure to about 30 psi (about 2 bar). The fuel flows through the pump solenoid control valve into the high pressure chamber. The solenoid control valve is controlled by an on-off signal generated by the MotoTron controller and synchronized with the motor position. The GDI high pressure pump is able to raise

the fuel pressure up to 250 bar. The fuel rail is a small aluminum alloy container. The injector is connected to the fuel rail through a fuel line. The pressure relief valve protects the whole system from damage due to excessive high pressure.

1.3.2 Control Block Diagram

In this thesis, a fuel rail pressure control system using a MotoTron control module is developed. In this study, the fuel rail control system consists of a MotoTron control module, a customized solenoid drive box, and a MotoTron control module host computer installed with MotoTune and LabVIEW. The MotoTron and the host computer communicate through the first CAN (controller area network) channel for real-time display and calibration. The LabVIEW GUI running on the host computer communicates with the MotoTron through the second CAN channel. Figure 3 shows the fuel rail pressure control system architecture.

Figure 3: Fuel Rail System Control Block Diagram

The fuel rail pressure control algorithm is developed in Simulink using a MotoHawk development environment that is capable of auto-coding, compiling, and real-time calibration. With the help of the MotoHawk development environment, the fuel pressure control algorithm can be developed efficiently, coded automatically from MATLAB/Simulink to "C", and compiled into the MotoTron production controller [8].

The control block diagram inside the MotoTron control module is shown in Figure 4. It includes the PI controller, dead-zone compensation, and feed-forward control. Each function

4

block in this control system is described in detail later. In addition, the control algorithm is also

discussed in detail with simulation and experimental results.
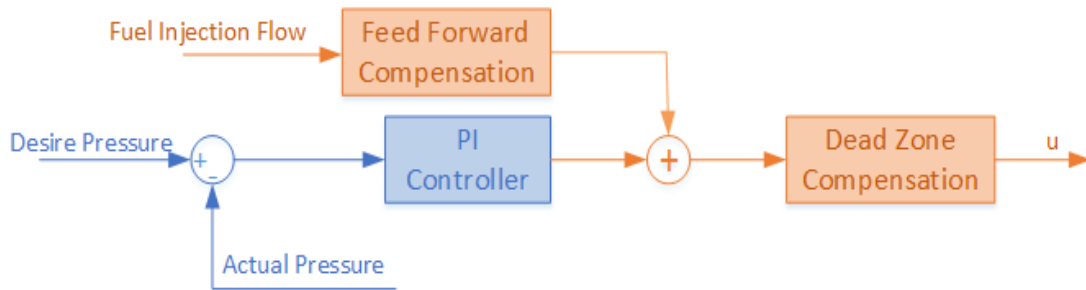
Figure 4: Control Block inside the MotoTron

1.3.3 MSU System Hardware

The high pressure fuel pump currently used in the MSU Energy and Automotive

Research Lab is a fuel cart produced by Pierburg Instruments Inc. as shown in Figure 5.
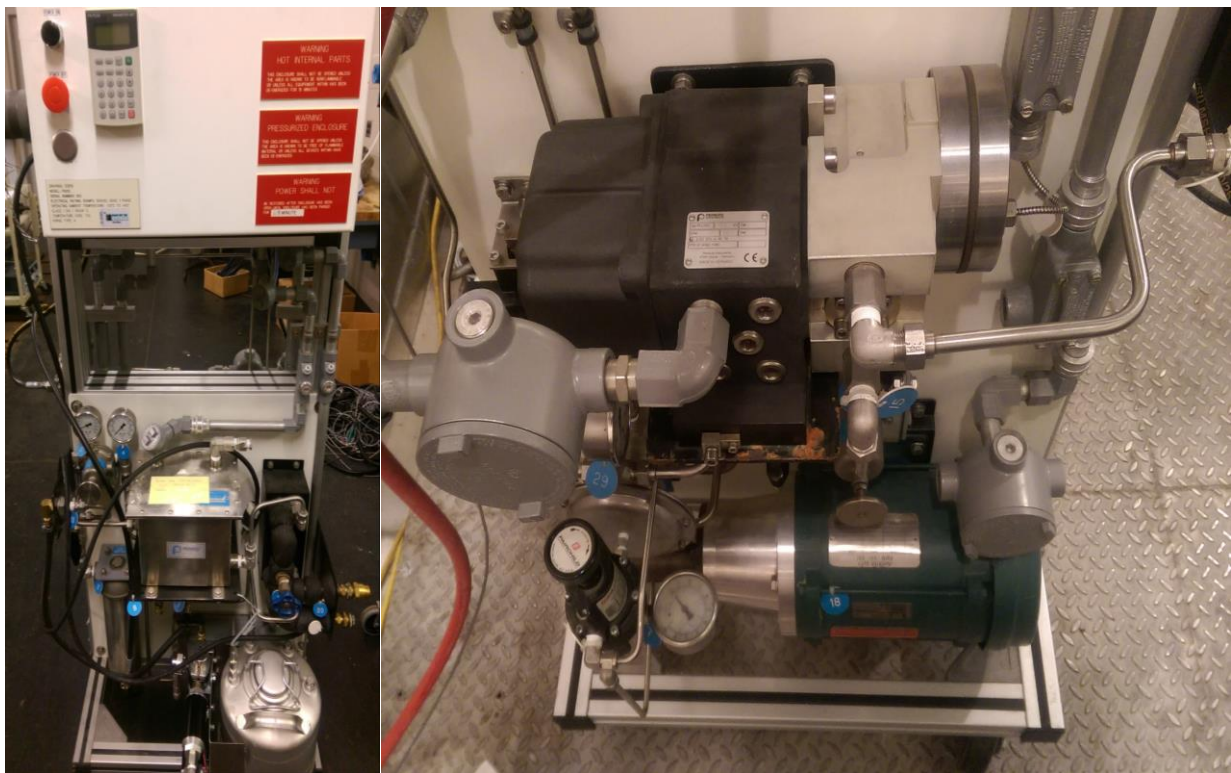
Figure 5: High Pressure Fuel Pump by Pierburg Instruments Inc.

The Pierburg fuel cart is able to provide the fuel rail pressure to 200 bar. To have an improved charge mixing, the required fuel rail pressure could exceed 200 bar and a new fuel rail system, shown in Figure 6, is developed to provide a fuel rail pressure up to 250 bar.
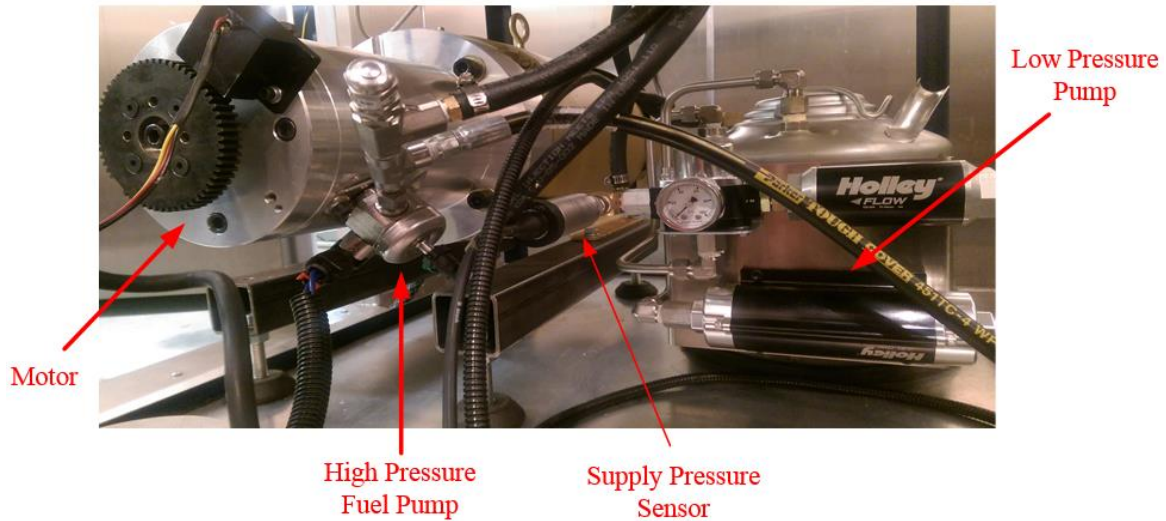
Figure 6: High Pressure Fuel Pump for 250bar

The new fuel system also contains a customized actuator drive box to control the pump solenoid, a host computer, and a MotoTron controller. Figure 7 shows the fuel rail pressure control system.
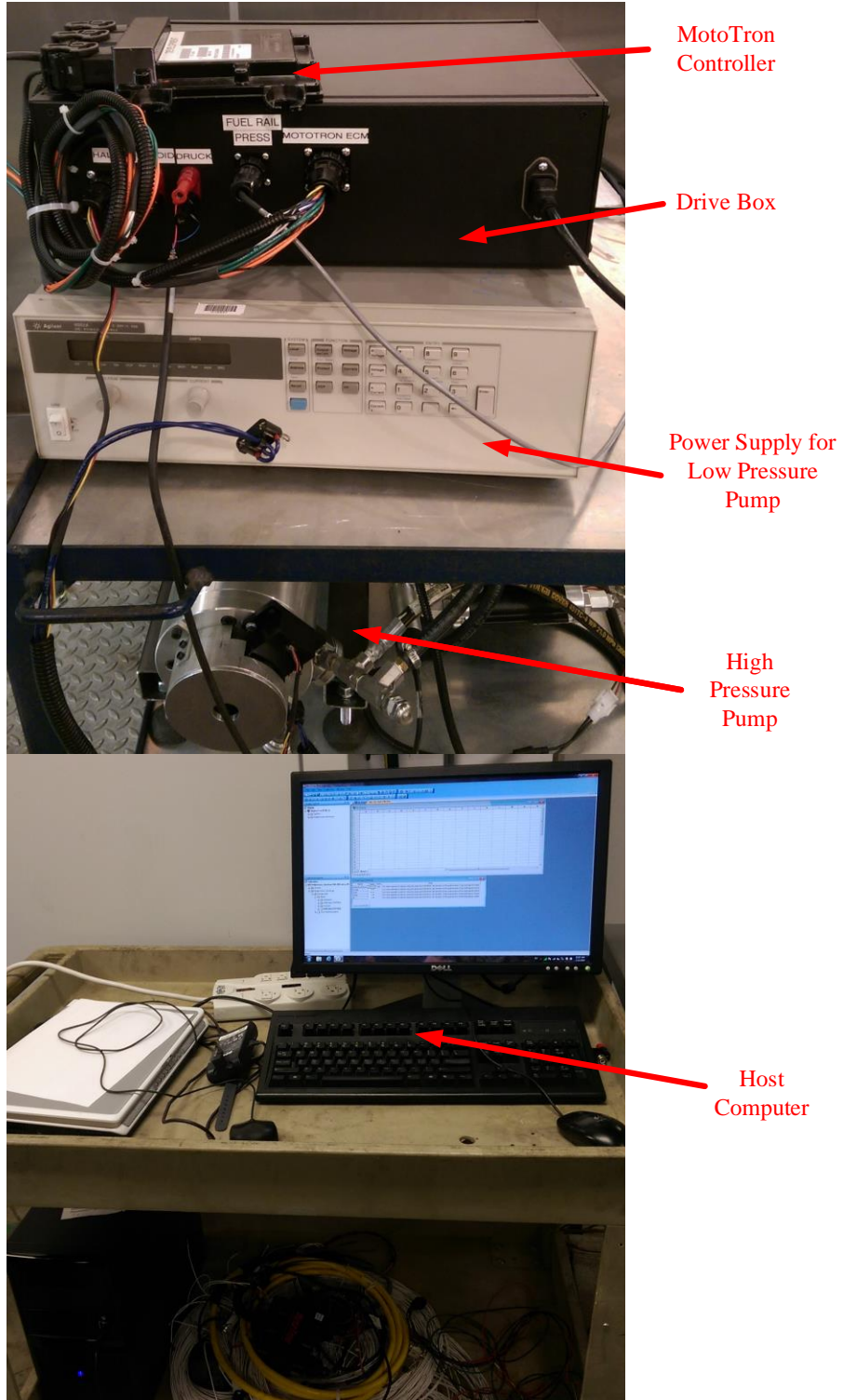
Figure 7: Fuel Rail Pressure Control System

CHAPTER 2: FUEL RAIL SYSTEM DEVELOPMENT

2.1 Introduction

A GDI engine requires a fuel system capable of providing stable high fuel pressure. In this thesis, a fuel rail pressure control system is developed using a MotoTron Controller. The MotoTron ECM (electronic control module) is synchronized with the motor position using a 60-2 tooth wheel and a hall-effect position sensor installed on the motor shaft. The pressure control system includes three blocks: I/O definition, fuel rail pressure management system, and CAN communication. A host computer is used for real-time calibration and control tuning. The fuel rail pressure control system diagram is shown in Figure 8.
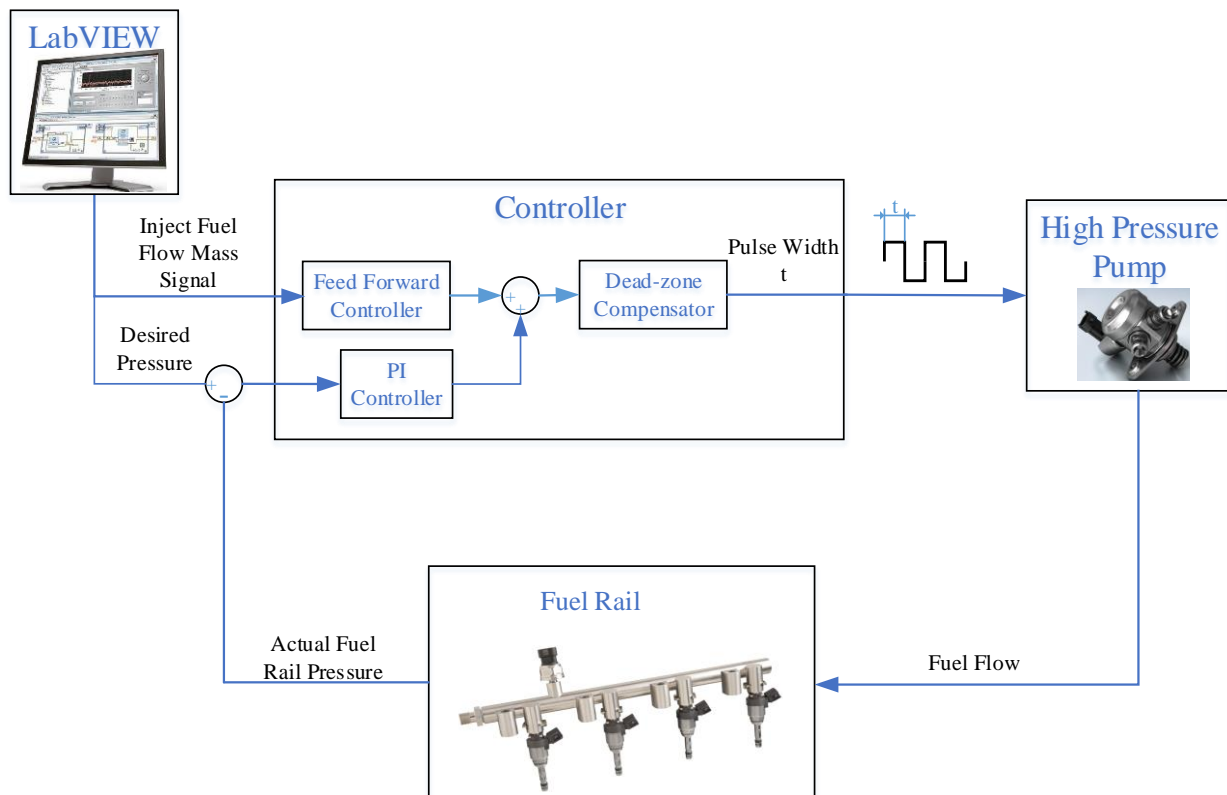
Figure 8: Fuel Rail Pressure Control System Diagram

The MotoTune is used for calibration and data recording. The intuitive, spreadsheet-like, user interface of the MotoTune makes it easy to access all of the calibration related RAM and ROM parameters contained in the ECM [9].

The GDI fuel pressure control system is an important part of the engine control system. The lab engine control system uses LabVIEW as the graphic user interface (GUI). In this thesis, in order to integrate fuel pressure control system into the engine control system, the fuel rail control system communicates with the engine control system through a CAN channel; and the required information are displayed on the engine control LabVIEW GUI [10]. In this way, users can tune the fuel pressure control parameters in real-time. And the fuel rail pressure is also displayed directly on the engine control LabVIEW GUI. In addition, the MotoTron fuel pressure controller communicates with the host computer to make it possible to use the MotoTune through a CAN link.

In this chapter, a mathematical control-oriented model of the fuel rail system is developed using MATLAB/Simulink. The main fuel rail system model is based upon the principle of fluid dynamics. The fuel leakage model is developed based on the experimental data and the injector model is based on the technical data of Bosch high pressure GDI fuel injector. The developed model is used to characterize the fuel rail system and to develop and validate the fuel pressure controller.

The control algorithm is also presented in this chapter. The fuel rail pressure control strategy consists of three main parts. They are a bumpless and anti-windup PI Controller, a feed-forward controller, and a dead-zone compensator. The bumpless and anti-windup PI and feed-forward controllers are used to minimize the pressure regulation error between the desired and

actual fuel rail pressures. The dead-zone compensation is used to prevent overheating the pump

solenoid control valve.

2.2 Experiment Equipment

2.2.1 Sensor and Actuator Signal Processing

Table 1 and Table 2 list the actuators and sensors used in the control system with their

signal definitions.

Table 1: Output Control Signal Definition

	Signal Definition	Type
1	Solenoid control	Position Synchronized PWM

Table 2: Input Control Signal Definition

	Signal Definition	Type
1	Crank position pulse	60-2 Hall Sensor
2	Enable/ Disable	Boolean
3	Fuel rail pressure	0~5 V
4	Supply pressure	0.88~4.4 V
5	Vcc sense	0~5 V
6	Injector Enable/ Disable	Boolean
7	SG_ COM_FuelMass_rk3	N/A
8	SG_ COM_FuelMass_rk2	N/A
9	SG_ COM_FuelMass_rk3	N/A

The pressure sensor for the low pressure pump is an industrial pressure transmitter (GE

Druck PTX 7200 Series) shown in Figure 9. Supply voltage for the sensor is 9-30 VDC; the

pressure range is 0-100 psi; and the output signal range is 4-20 mA.

Figure 9: Druck PTX 7200 Series Industrial Pressure Transmitter

The pressure sensor wire diagram is shown in Figure 10, which leads to a transfer function for the low pressure sensor as follows:

$$P = \frac{U}{220} \times \frac{25}{4} \times 1000 - 25 \qquad (1)$$
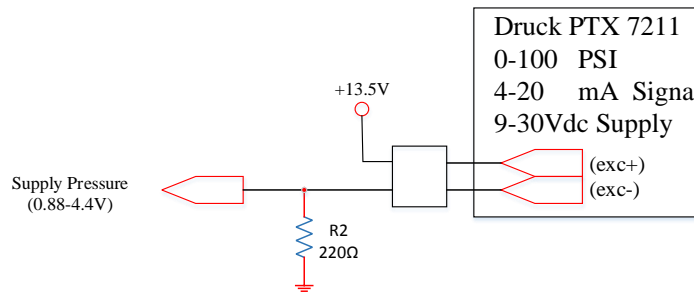
Figure 10: Supply Pressure Sensor Wire Diagram

The pressure sensor used for rail pressure is a Chrysler production GDI fuel pressure sensor shown in Figure 11.

Figure 11: Chrysler Fuel Sensor

11

The high fuel pressure sensor wire diagram is shown in Figure 12.
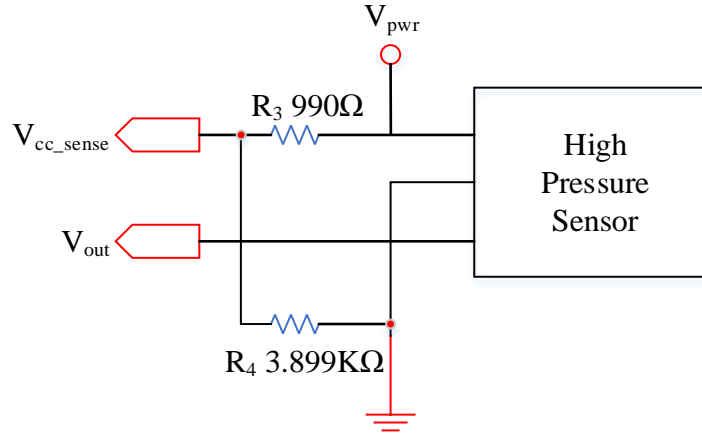
Figure 12: High Pressure Sensor Wire Diagram

The power supply voltage for the sensor is 4.75-5.25 VDC. The operational pressure range is between 0 and 300 bar. The associated transfer function of the sensor is

$$(V_{out}/V_{pwr}) \times 100 = 0.26667 \cdot P(bar) + 10 \tag{2}$$

where

$$V_{pwr} = \frac{V_{cc}(R_3 + R_4)}{R_4} \tag{3}$$

2.2.2 MotoTune

The MotoTune software provides all of the functionalities needed for typical calibration tasks. During the system development, the MotoTune is used to display the sensor and control parameters in real-time and record associated data. More importantly, it is used to input real-time control commands and calibrations. The MotoTune interface is shown in Figure 13.
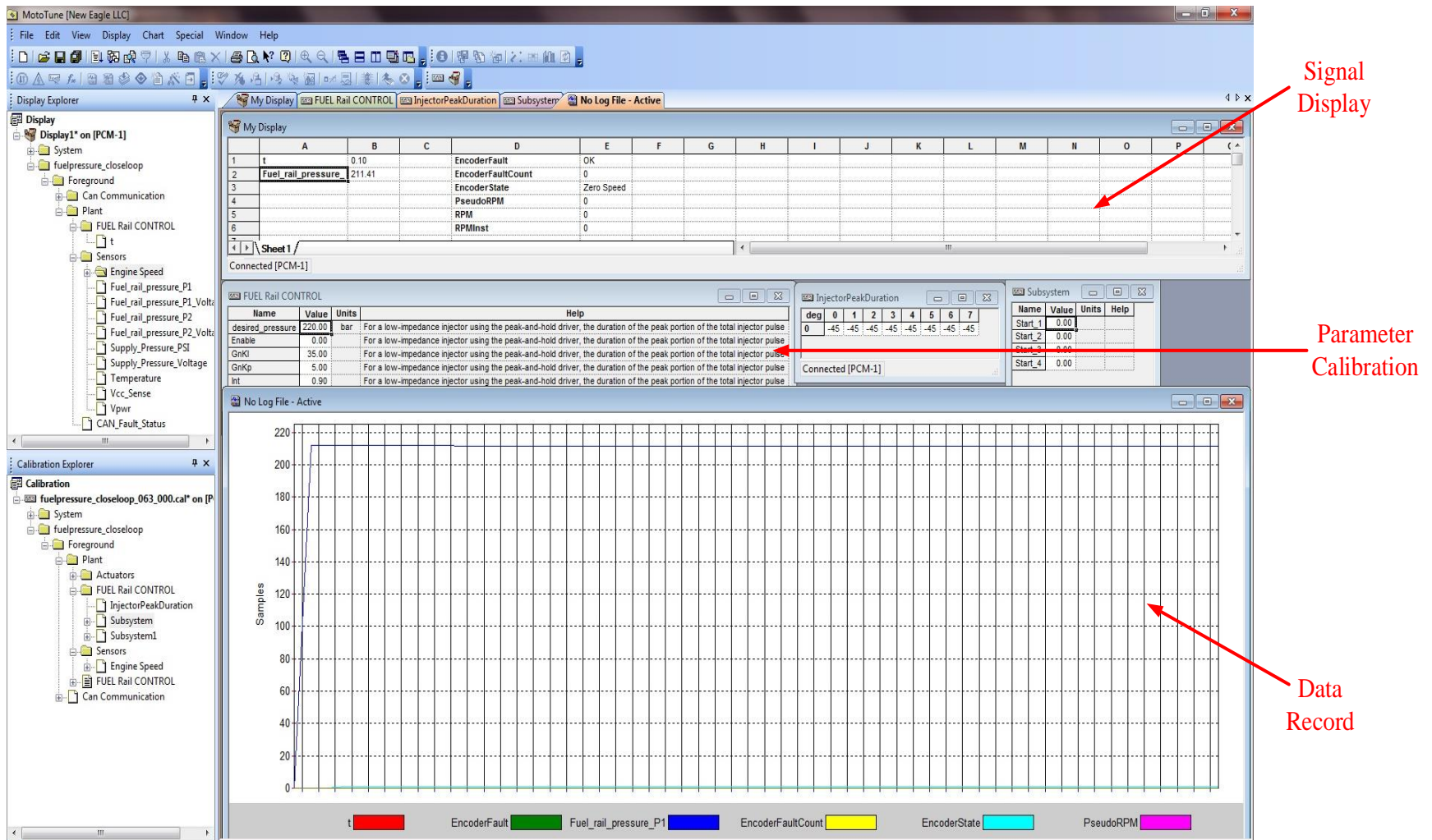
Figure 13: MotoTune Interface

2.2.3 CAN Communication

CAN communication is very important in the fuel pressure control system. In this research, the first CAN channel is used to compile the auto-coded control algorithm into the MotoTron control module. The MotoTron control module communicates with other devices through the second CAN channel as shown in Figure 14. The fuel rail pressure controller sends the control variables, such as pump speed and fuel rail pressure, to the engine controller and display on the engine controller LabVIEW GUI. Meanwhile, the fuel pressure controller can also read the commands from the host computer to calibrate the PI gains and set reference fuel rail pressure. The CAN link between the engine control host computer and the MotoTron controller is through an NI high-speed USB cable.
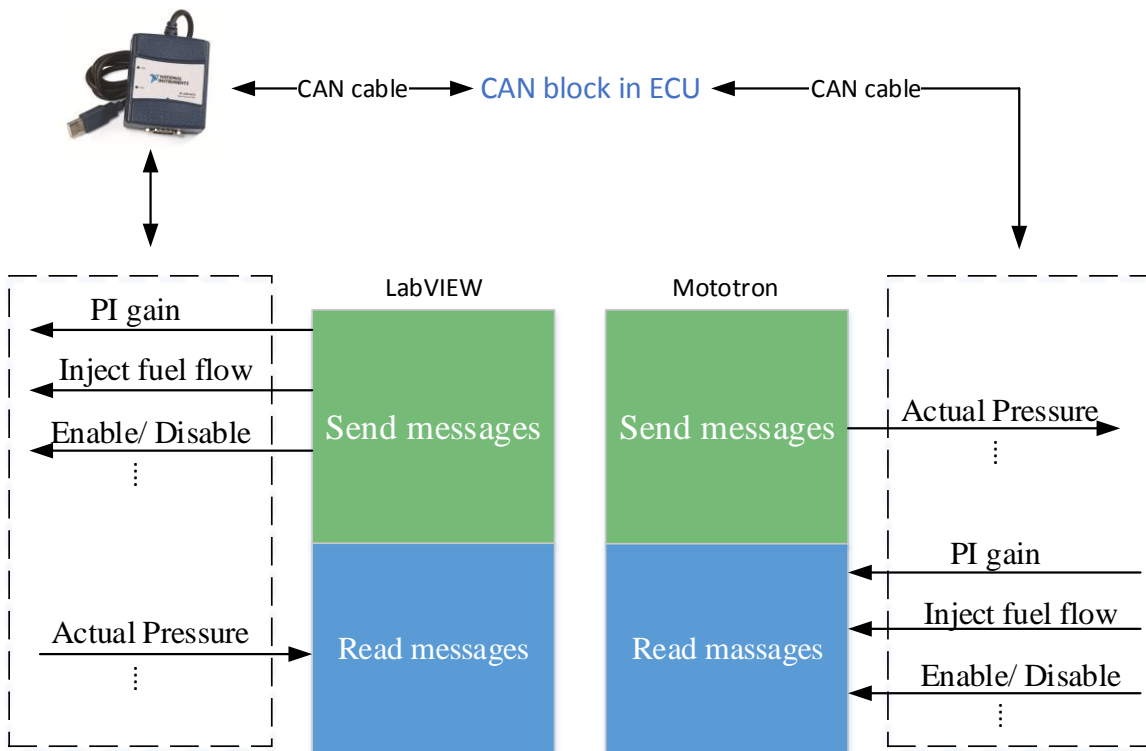
Figure 14: CAN Communication

2.2.4 LabVIEW GUI Development

The engine control host computer runs NI LabVIEW GUI. Part of the engine control GUI interface is used to monitor the fuel rail system status, display the control parameter and sensor values, and provide real-time control commands.

The fuel rail system provides the desired fuel rail pressure for the engine system and it is a part of the entire engine system. Although the fuel rail and engine control systems use different MotoTron control modules, the entire engine system is monitored and controlled using the same LabVIEW GUI. The monitoring page of the engine control LabVIEW GUI is shown in Figure 15.
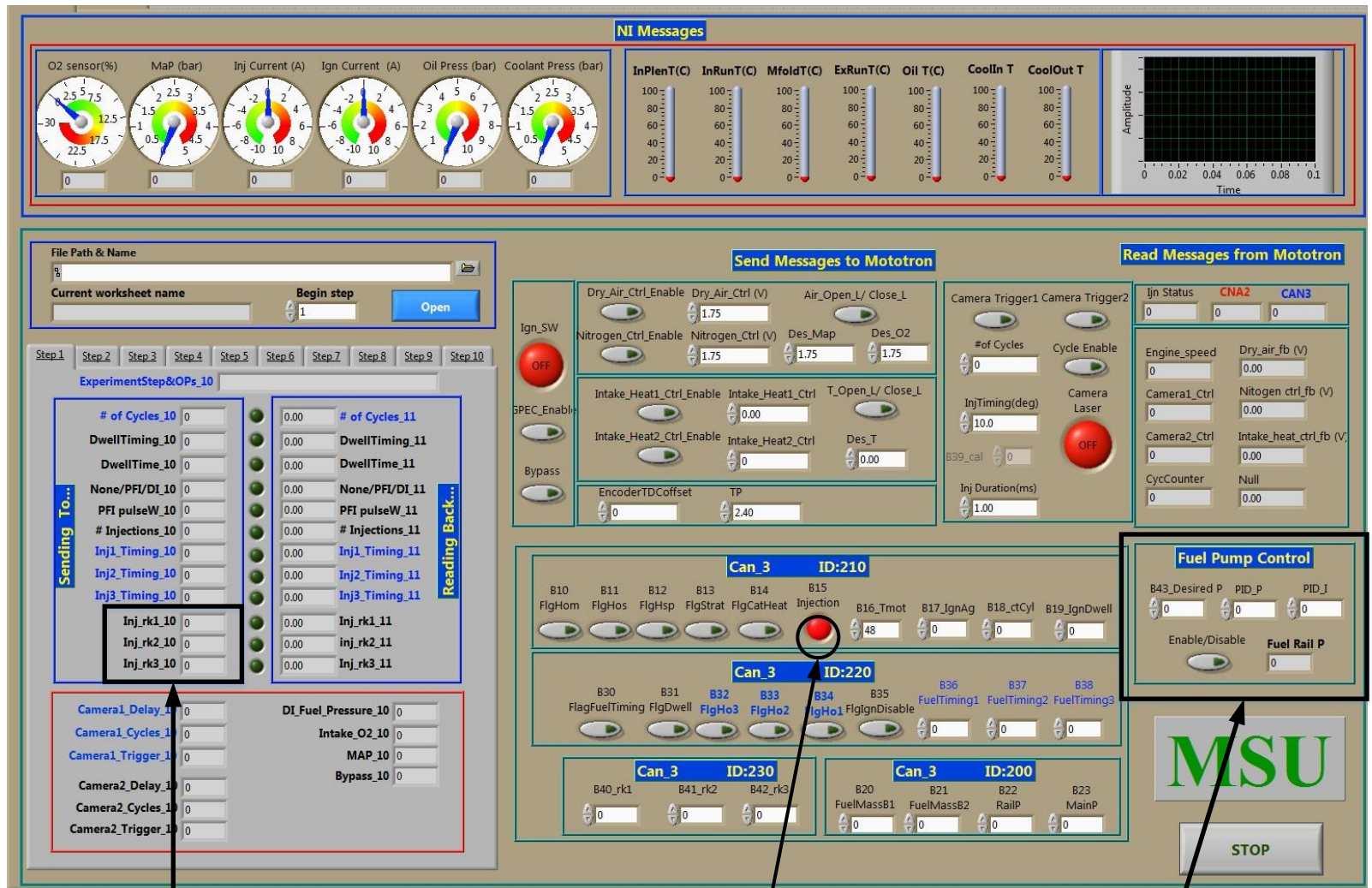
Figure 15: LabVIEW GUI

2.3 Fuel Rail System Modeling

2.3.1 High Pressure Pump Model

The gasoline direct injection high pressure pump is a single-cylinder, radial-piston pump driven by a camshaft through a roller tappet installed on the engine cam shaft. For this study, the pump is mounted on the electrical motor shaft (simulated cam shaft). The pump is driven by the motor shaft with 4 lobes; see Figure 16 for its dimensions.
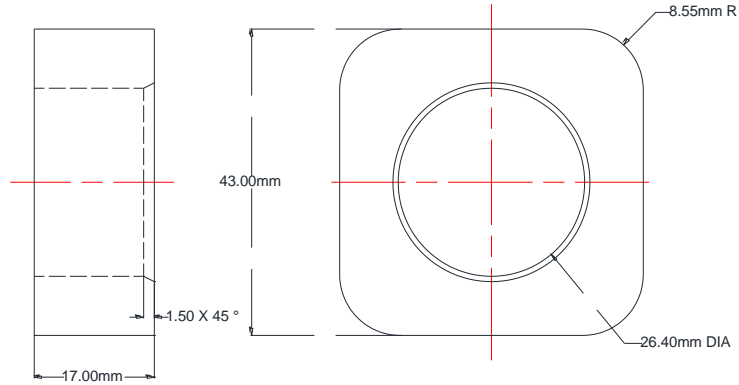
Figure 16: Cam Dimension

The pump piston displacement h is dependent on the cam dimension. Let θ be the camshaft angular position. When $\quad 0 \le \theta \le \arctan \dfrac{12.95}{21.5}$

$$h = \frac{21.5}{\cos \theta} - 21.5 \tag{2}$$

when $\arctan \dfrac{12.95}{21.5} < \theta < \dfrac{\pi}{4} + \arctan \dfrac{12.95}{21.5}$

$$h = \sin\left(\pi - \left(\frac{\pi}{4} - \theta\right) - \arcsin\left(\frac{12.95\sqrt{2}\sin\left(\frac{\pi}{4} - \theta\right)}{8.55}\right)\right) \times \frac{8.55}{\sin\left(\frac{\pi}{4} - \theta\right)} \tag{3}$$

and when $\quad \dfrac{\pi}{4} + \arctan \dfrac{12.95}{21.5} \le \theta < \dfrac{\pi}{2}$

17

$$h = \frac{21.5}{\cos\left(\frac{\pi}{2} - \theta\right)} - 21.5 \qquad (4)$$

The piston displacement, described by equations (2) to (4) is shown in Figure 17.
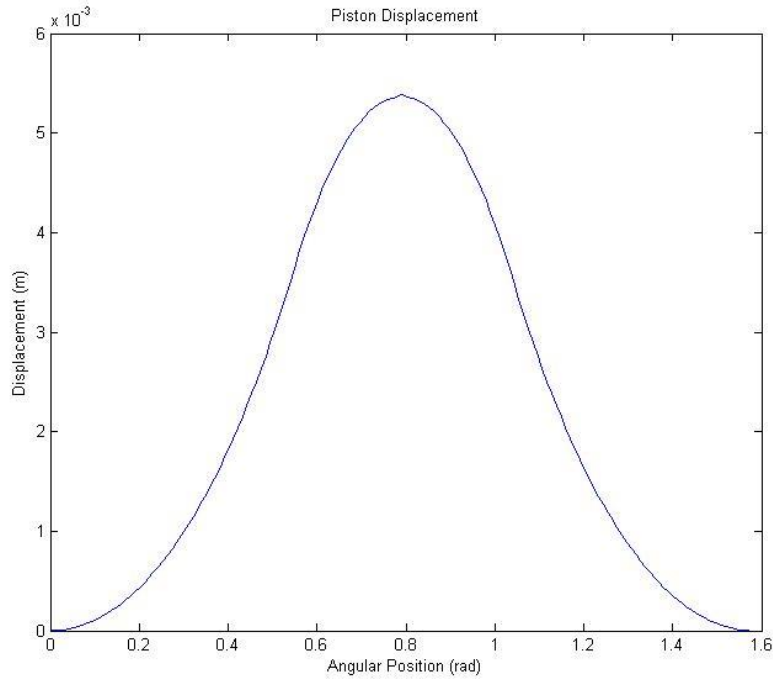
Figure 17: Piston Displacement

In the model, the basic principle of the fuel is expressed by the bulk modulus of elasticity (see [11])

$$K_f = -\frac{dp}{dv/v} = \frac{dp}{d\rho/\rho} \qquad (5)$$

where K_f is the bulk modulus of elasticity defined as the ratio of the pressure increment to the resulting relative decrement of the volume and K_f and p have the same units bar. Parameter dp is the differential change in pressure; dv is the differential change in volume; V is the initial volume; $d\rho$ is the differential change in density; and ρ is initial density. Under normal operating

conditions K_f is set to 12,000 bar and its relationship to fuel pressure p (bar) can be expressed as follows [12]:

$$K_f = 1.2 \cdot 10^4 \cdot \left[1 + 0.6 \frac{p}{600} \right] \qquad (6)$$

From equation (5), the relationship between the rate changes of pressure and volume can be obtained.

$$\frac{dp}{dt} = -\frac{K_f}{v} \cdot \frac{dv}{dt} \qquad (7)$$

The rate change of fuel pressure for the high pressure pump can be written as

$$\dot{p}_p = -\frac{K_f(p_p)}{v_p(\theta)} \left(\frac{dv_p}{dt} - q_u + q_{pr} + q_L \right) \qquad (8)$$

where $\dfrac{dv_p}{dt}$ is the fuel volume change due to piston motion.

$$\frac{dv_p}{dt} = \frac{dA_p \cdot h_p(\theta)}{dt} = A_p \frac{dh_p}{dt} = A_p \frac{dh_p}{d\theta} \cdot \frac{d\theta}{dt} \qquad (9)$$

$$\theta = \omega_{rpm} \cdot t = RPM \cdot \frac{2\pi}{60} \quad rad\!\!\Big/\!\!_s \qquad (10)$$

According to equation (10), we can have

$$\frac{d\theta}{dt} = \omega_{rpm} = RPM \cdot \frac{2\pi}{60} \qquad (11)$$

So equation (9) can be rewritten as

$$\frac{dv_p}{dt} = A_p \cdot RPM \cdot \frac{2\pi}{60} \cdot \frac{dh_p}{dt} \qquad (12)$$

where $v_p(\theta)$ is the instantaneous volume of the high pressure pump due to piston motion and it can be calculated by

$$v_p(\theta) = V_p^0 - A_p \cdot h_p(\theta) \tag{13}$$

Note that V_p^0 is the cylinder total volume at BDC and A_p is the section of the pump piston.

Let $q_u \left(m^3 s^{-1} \right)$ be the intake fuel flow of the high pressure pump, $q_{pr} \left(m^3 s^{-1} \right)$ the intake fuel flow of the fuel rail, and $q_L (m^3 s^{-1})$ the leakage fuel. And $q_u (m^3 s^{-1})$ can be calculated by applying the energy conservation law as follows:

$$q_u = \mathrm{sgn}(p_t - p_p) \cdot c_d \cdot (U \cdot A_{tp}) \cdot \sqrt{\frac{2|p_t - p_p|}{\rho}} \tag{14}$$

where $P_t (bar)$ is the supply pressure from the low pressure pump; $\mathrm{sgn}(P_t - P_p)$ is the sign function defining the flow direction; A_{tp} is the intake orifice section area of the high pressure pump and ρ is the gasoline density (0.73kg/L). For this study c_d is the coefficient defined as the ratio of the actual discharge to the theoretical discharge [13] and is chosen to be 0.6. Note that U is the state of the solenoid control valve. When the valve is closed, $U = 0$; and when the valve is open, $U = 1$.

2.3.2 The Fuel Rail

The fuel rail contains a certain volume of gasoline fuel. The time derivative of fuel pressure in the fuel rail can be written as

$$\dot{p}_r = \frac{K_f(p_r)}{v_r} \left(q_{pr} - q_l - q_{ri} \right) \tag{15}$$

where v_r is the volume of the fuel rail; $q_l (m^3 s^{-1})$ is the leakage due to the pressure relief valve; $q_{ri} (m^3 s^{-1})$ is the fuel injection flow rate; and $q_{pr} \left(m^3 s^{-1} \right)$ is the intake fuel flow of the fuel rail. Since there is a check valve between the fuel rail and the high pressure fuel pump, the fuel

cannot flow back to the outlet of the high pressure pump. Therefore the intake flow can be expressed as follows:

$$q_{pr} = \begin{cases} c_d \cdot (U \cdot A_{pr}) \cdot \sqrt{\dfrac{2(p_p - p_r)}{\rho}} & p_p > p_r \\ 0 & p_p \le p_r \end{cases} \tag{16}$$

where A_{pr} is the intake orifice section area of the fuel rail.

2.3.3 Fuel Injector and Leakage

The fuel injection flow q_{ri} and fuel leakage q_l are considered as perturbations of the fuel rail system and they are determined experimentally.

2.3.3.1 Fuel Injector

The fuel injector used in the GDI engine for this study is the high-pressure piezo injector HDEV4 made by Bosch; see Figure 18.

Figure 18: BOSCH High-pressure Piezo Injector HDEV4

The fuel injector has a high evaporation rate, low penetration, and large metering range. With this injector, the GDI engine is able to generate the desired air-fuel mixture directly in the combustion chamber. The technical features of the injector are shown in Table 3.

Table 3: The Technical Features of the Injector

Needle actuation	Direct
Spray angle	85°±5°
Shot-to-shot scatter	±1°
Back-pressure dependence	<4%
Droplet size SMD (Sauter Mean Diameter)	10-15 μm
Penetration	< 30 mm
Needle lift	≤ 35 μm
Partial-lift capability	≥ 10-35 μm
Injection time	70-5000 μs
Multiple injection	≤ 5 injections/cycle
Interval time	≥ 50 μs
Metering range	0.5-150 mg/injection

The dynamic flow range of the injector is q_{dyn} (34.5mg/lift @ t=1ms). For the test engine,

there are 3 injections available for each combustion event as shown in Table 4.

Table 4: Injection Signals

Function	Name	Units
DI Fuel Mass	Injection1	%
	Injection2	%
	Injection3	%

The total injection flow can be calculated by

$$q_{ri} = (Injection1 + Injection2 + Injection3) \cdot q_{dyn} \tag{17}$$

2.3.3.2 Leakage

The leakage flow is caused by the pressure relief valve used to prevent over-pressurizing

the fuel system. When the pressure is lower than 200 bar, the leakage flow is very small and can

be neglected. When the pressure is higher than 200 bar, the relationship between leakage flow

and pressure are nonlinear. In the model, the leakage flow is calculated by using a lookup table that represents the nonlinear relationship between the pressure and leakage flow. The data in the lookup table were determined experimentally and they are shown in Figure 19.
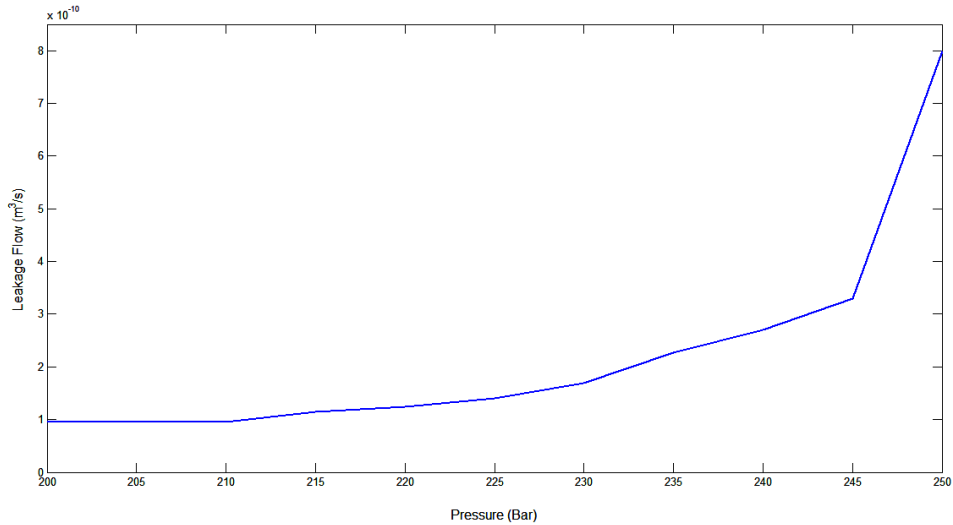

Figure 19: Relationship between the Leakage and the Pressure

2.4 Fuel Pump Control

2.4.1 Control Principle

The open-loop control strategy of the high pressure fuel pump is shown in Figure 20. The cam is driven by the electrical motor shaft (simulated cam shaft) so that the piston of the high pressure fuel pump moves up and down. For safety reasons, the solenoid control valve inside the pump is normally open. When the piston moves downward from the top dead centre (TDC) to the bottom dead centre (BDC), the fuel flows into the high pressure fuel pump from its intake port due to the pressure difference. The demand control valve inside the high pressure pump is activated by the solenoid so that the flow volume can be regulated between zero and maximum delivery. When the piston moves upwards from BDC to TDC, the solenoid control valve is closed for a certain time period t that is the control variable for the fuel pressure control system.

During this time period, the piston goes up and pushes the fuel from the outlet into the fuel rail. After this time period, the solenoid control valve opens again. Due to the check valve between the fuel pump and rail, the fuel cannot flow back to the outlet, the fuel pressure inside the fuel rail can be maintained. Since the piston keeps moving up due to the pressure difference, the fuel flows back to the fuel tank from the high pressure pump through the intake valve.
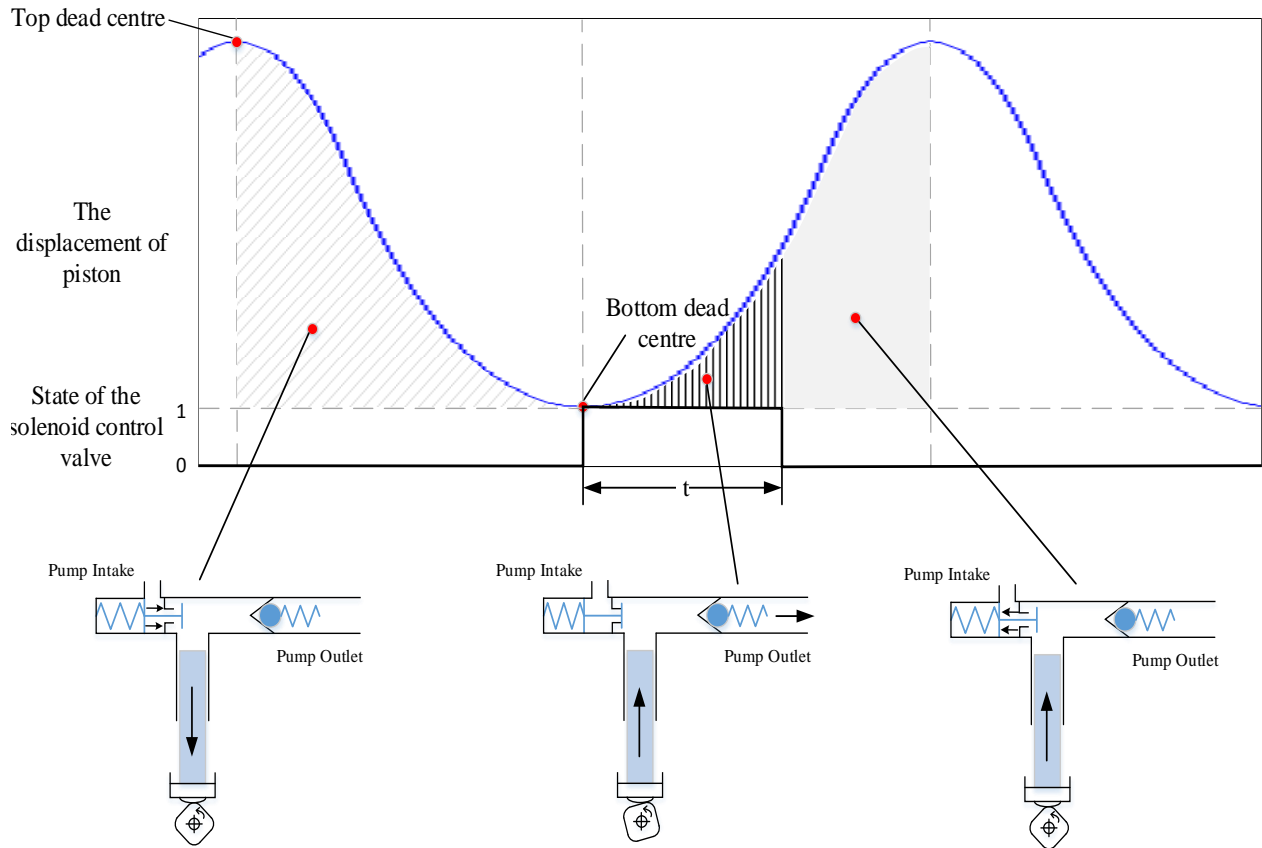
Figure 20: Control Principle of the High Pressure Fuel Pump

The whole fuel pump system is synchronized with the motor shaft position signal. Since a MotoTron engine controller is used for fuel pump control, one engine cycle in the MotoTron is 720°. For our case the pump is mounted on the equivalent crankshaft with each rotation equal to 360°, which leads to four strokes for the fuel pump. Within one engine cycle in the MotoTron control module, 8 control pulses need to be generated for the pump solenoid valve as shown in

Figure 21. Channel 1 (C1), the yellow signal, is the simulated cam position signal (one pulse per engine cycle); channel 2 (C2), the pink signal, is the electric motor shaft position (simulated crank) single (60-2 tooth); and channel 3 (C3), the blue signal, is the generated control pulse signal for the solenoid control valve. The pulse width is the control variable that will be defined by the output of the duel rail pressure controller. In this study, the dSPACE engine simulation system is used to simulate the crank position pulse signal with 60-2.
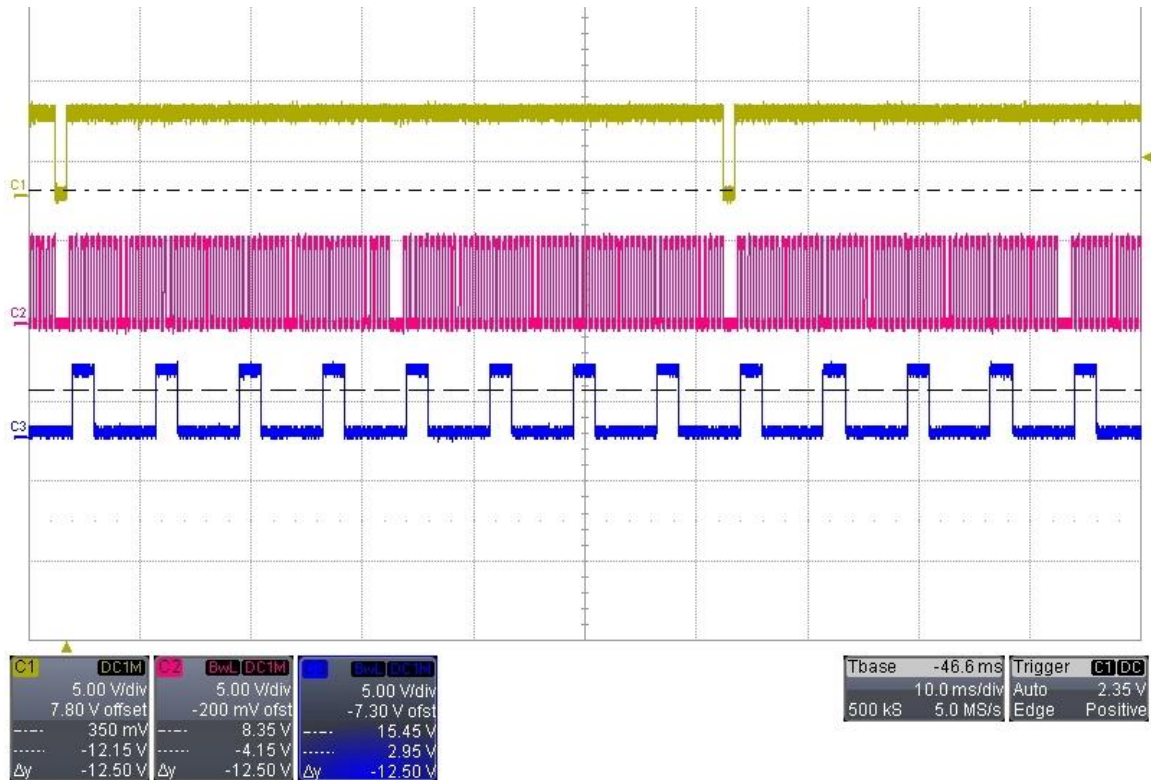
Figure 21: Pulse Signal for Solenoid Control Valve Synchronized with Crank Position Pulse

To have high pumping efficiency, the rising edge of the solenoid valve control pulse should begin at the pump BDC. The control pulse without proper calibration is shown in Figure 22.
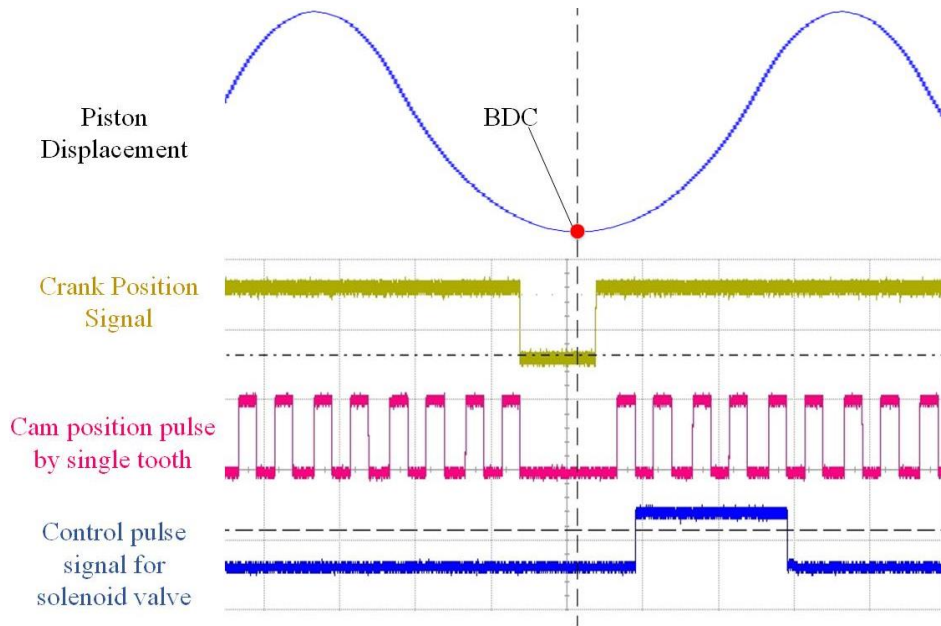
*Figure 22: Pulse Signal for Solenoid Control Valve before Calibration*

The BDC location is determined after the pump is installed onto the motor shaft. From Figure 22, the start of the pulse signal is obviously after the BDC. By moving the pulse signal forward the rising edge can be in-line with the BDS as shown in Figure 23.
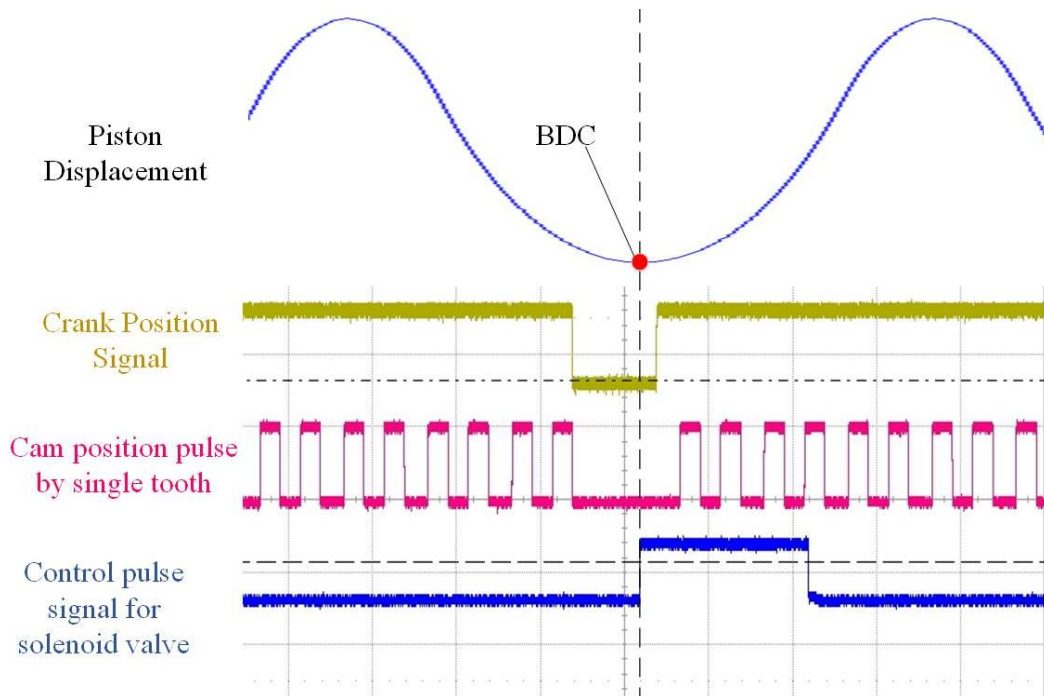

Figure 23: Pulse Signal for Solenoid Control Valve after Calibration

2.4.2 Open-Loop Control

The open-loop control system, shown in the Figure 24, does not include any feedback signal.


Figure 24: Open-loop Control System

Although the open-loop control cannot correct any pressure regulation errors and compensate for disturbances in the fuel system, it was used to observe the relationship between the control input and pressure response. The open-loop control test results are used to generate certain calibrations for the closed-loop controller.

2.4.3 Closed-Loop Control

The closed-loop control aims to minimize the error between the actual fuel rail pressure and the desired (reference) pressure. The closed-loop control system structure is shown in Figure 25. The closed-loop controller in this research contains a PI controller with the dead-zone compensation.
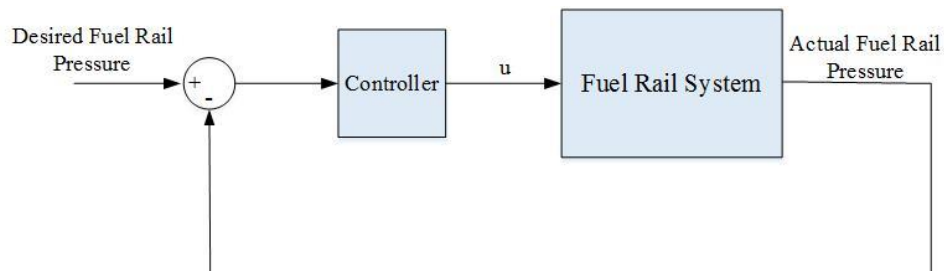

Figure 25: Closed-loop Control System

2.4.3.1 PI Controller

In this study, a bumpless anti-windup PI controller is used to control the fuel rail pressure. The PI controller is shown in Figure 26. The feed-forward block of this PI controller can be used for future feed-forward control. The proportional gain block of the PI controller includes a bumpless gain feature, which limits the rate of change of the proportional gain to provide smooth gain scheduling; and the PI control system further includes anti-windup logic to disable the PI integrator if the actuator drive signal is upper or lower bounded and the error signal is greater or less than zero respectively, thereby creating dynamic saturation of the PI integrator [14].
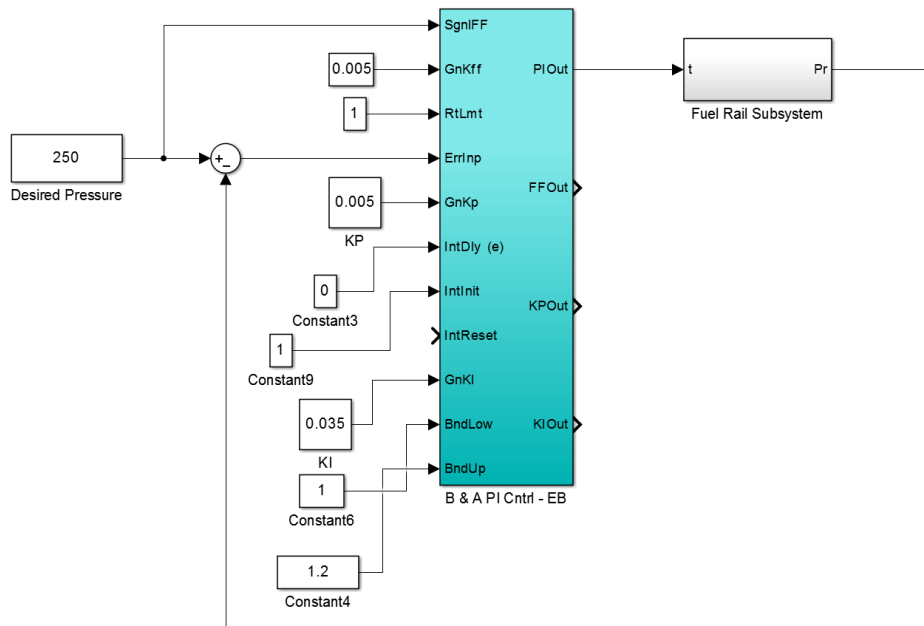
Figure 26: Bumpless and Anti-windup PI Controller

The solenoid drive circuit has a 1.0 ms precharge feature to improve the repeatability of the pump solenoid valve and it is validated during the open-loop control test. That is, when the pulse width is smaller than 1.0 ms, the solenoid control valve does not react to the control pulse. Therefore, the control pulse lower and upper bonds are set to 1.0 and 1.2 ms respectively to avoid the PI controller integrator over flow and reduce pressure overshoot.

2.4.3.2 Dead-zone Compensation

Due to the electro-magnetic property of the solenoid valve, it takes about 0.3 ms to open after the pulse rising edge; and it takes even more time to close the solenoid control valve. The time delay between the open and close of the solenoid control valve is defined as the dead-zone shown in Figure 27.
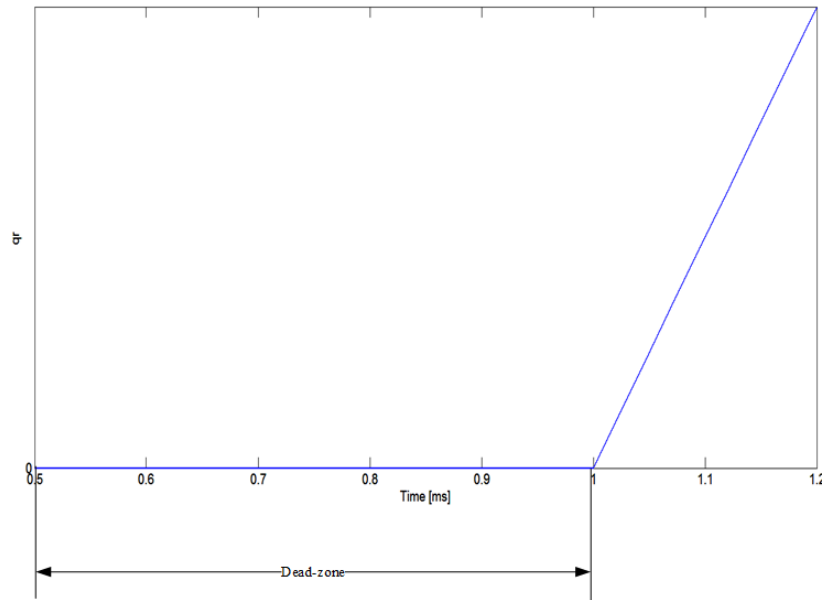

Figure 27: Dead-zone Definition

As a summary, when the control pulse width is smaller than 1ms, the solenoid valve will not open, but there is current flow through the solenoid winding, which could increase the solenoid winding temperature. The dead-zone compensation is to set the pulse width to 0.1 ms when the PI control pulse width is smaller than 1 ms and the output is equal to the PI control pulse width when the PI control is greater than or equal to 1 ms.

The seventh and eighth inputs (IntInit and IntReset) in the bumpless and anti-windup PI controller are used to implement the dead-zone compensation. IntReset is connected with the enable/disable of the solenoid control pulse signal. The input of IntInit was set as 1.0 ms so that the PI controller responds faster.

2.4.4 Feed-forward Control

Feed-forward control is used to compensate the fuel leakage and injection flow. If the PI controller consisted of the bumpless and anti-windup feature with dead-zone compensation, the fuel rail pressure would fluctuate significantly. For example, when the desired pressure is 200 bar, the actual fuel rail pressure fluctuation is shown in Figure 28, where the large decreasing of the fuel pressure is caused by the start of fuel injection. Figure 28 shows that the fuel rail pressure drops around 12 bar after fuel injection starts and the control system response is slow without feed-forward control. Although the pressure is stable at the steady state with an error between the reference and actual fuel rail pressure less than 2%, the huge pressure drop needs to be avoided. By adding the feed-forward control, the fuel rail pressure fluctuation during the transient operation can be improved significantly.
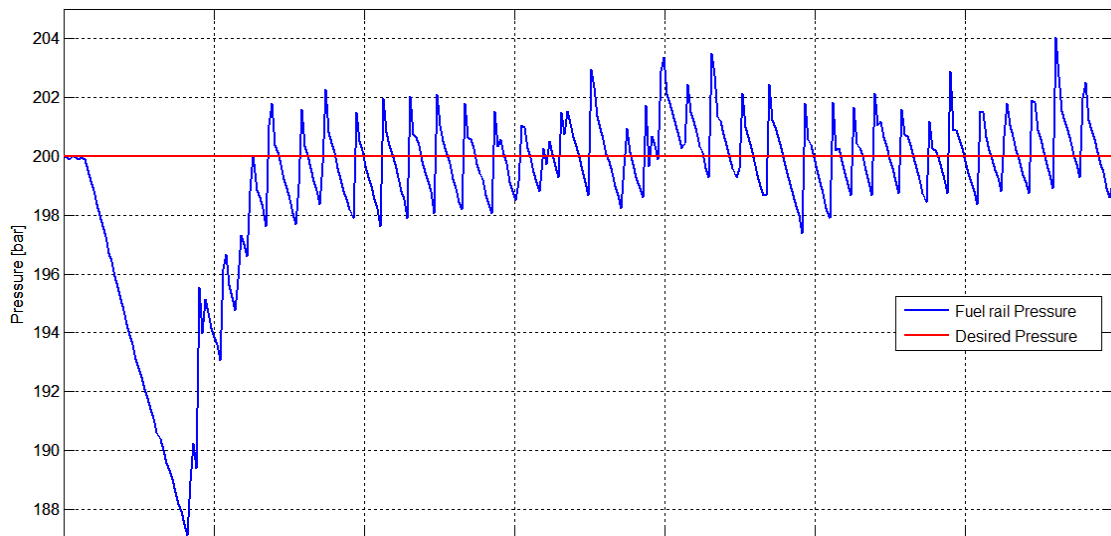

Figure 28: Experiment Data of the Pressure Performance of the System without Feed-forward

Control with injection

The feed-forward controller attempts to compensate the fuel leakage and injection flow. The max flow injection quantity is 4.7×10^{-8} m^3 per lift at 1ms. The volume change due to piston motion is shown in Figure 29.
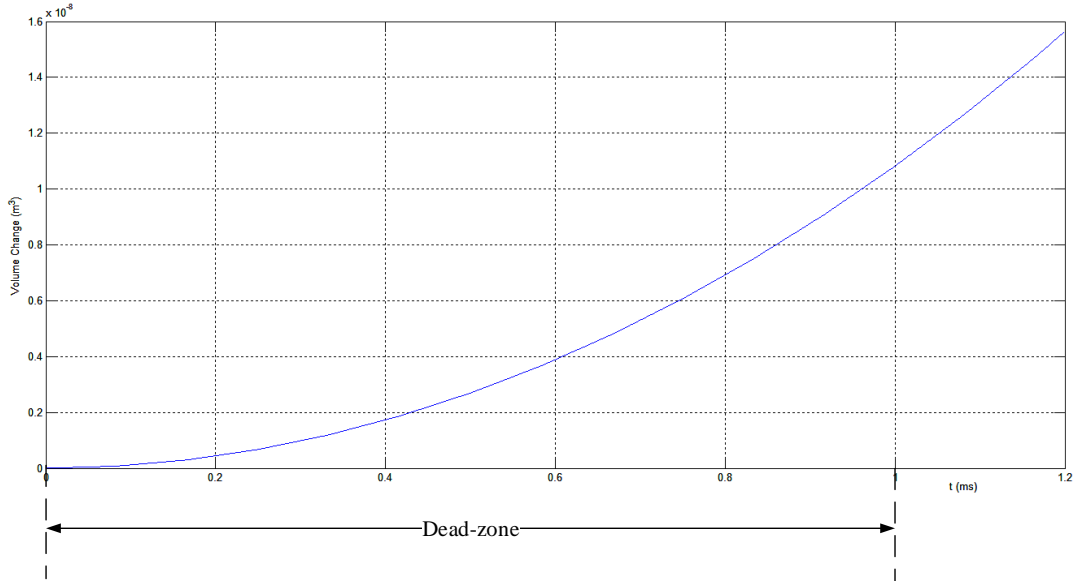
Figure 29: Volume Change due to Piston Motion from 0 to 1.2ms

Because of the dead-zone, the solenoid is active only from 1 ms to 1.2 ms. Hence, the maximum volume of the flow from the pump to the fuel rail is $0.48 \times 10^{-8} m^3$ per pulse. According to the relationship between piston position and output flow volume, a feed-forward lookup table, shown in Table 5, can be designed. For every simulated engine cycle, there are eight pulses to control the solenoid control valve to compensate the injection volume. When the injection flow volume increases, the pulse width can exceed 1.2 ms.

Table 5: Lookup Table for Feed-forward Control

Compensation Flow Volume (m^3)	Pulse width (ms)
0	1
0.0454×10^{-8}	1.02
0.0908×10^{-8}	1.04
0.1362×10^{-8}	1.06
0.1817×10^{-8}	1.08
0.2302×10^{-8}	1.10
0.2794×10^{-8}	1.12

Table 5 (cont'd)

0.3286×10^{-8}	1.14
0.3777×10^{-8}	1.16
0.4294×10^{-8}	1.18
0.4824×10^{-8}	1.20

CHAPTER 3: SIMULATION VALIDATION

3.1 Introduction

Simulation validation of the developed simulation model is conducted during the model development process to ensure the model accuracy [15]. The model was developed using these parameters measured on the actual fuel rail system and calibrated by comparing the Simulink model response with the experimental data.

Two different operating conditions are simulated to validate the control law: one is for tracking validation and another for tracking with injection flow. These two validation conditions are also repeated in the experiments. The Simulation results show that the fuel rail control system is able to maintain the fuel rail pressure with or without fuel leakage and injection flow disturbances.

Before the controller could be used on the actual fuel rail system, it should be validated using the simulation model. After the model was developed, the simulation and experiment data were compared, which is described in the next Chapter.

3.2 Model Validation

Simulation validation is utilized to determine if the developed model is an accurate representation of the actual system [16]. To test the fuel rail pressure, a fuel rail plant model was established in Simulink. The parameters of the fuel rail system are shown in Table 6. With these parameters, the fuel rail system Simulink model is able to replicate characteristics of the actual fuel rail system.

Table 6: The Parameters in GDI Fuel Rail System Simulink Model

The section of the inlet in high pressure pump (m^2)	1.69×10^{-5}
The section of the inlet in fuel rail (m^2)	1.65×10^{-5}
The section of the pump piston (m^2)	6.33×10^{-5}
The max volume of the high pressure pump (m^3)	8.7×10^{-7}
The pressure supplied by low pressure pump (psi)	32
Solenoid valve delay time (ms)	2.5
The volume of fuel rail (m^3)	8.3×10^{-5}
Motor Speed (RPM)	1200
Density of the Gasoline (kg/L)	0.73

The fuel rail Simulink model is shown in Figure 30. The block diagram of the closed-

loop fuel rail system with the controller is shown in Figure 31.
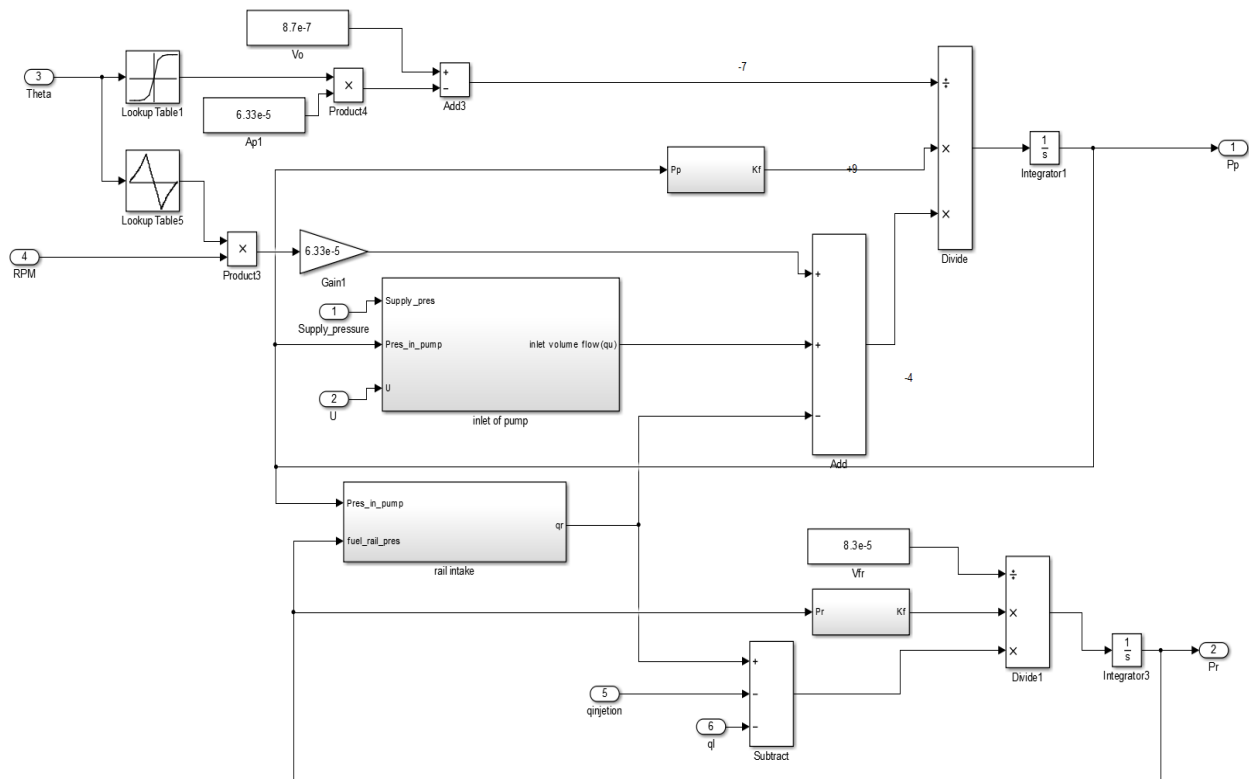
*Figure 30: Fuel Rail System Simulink Model*
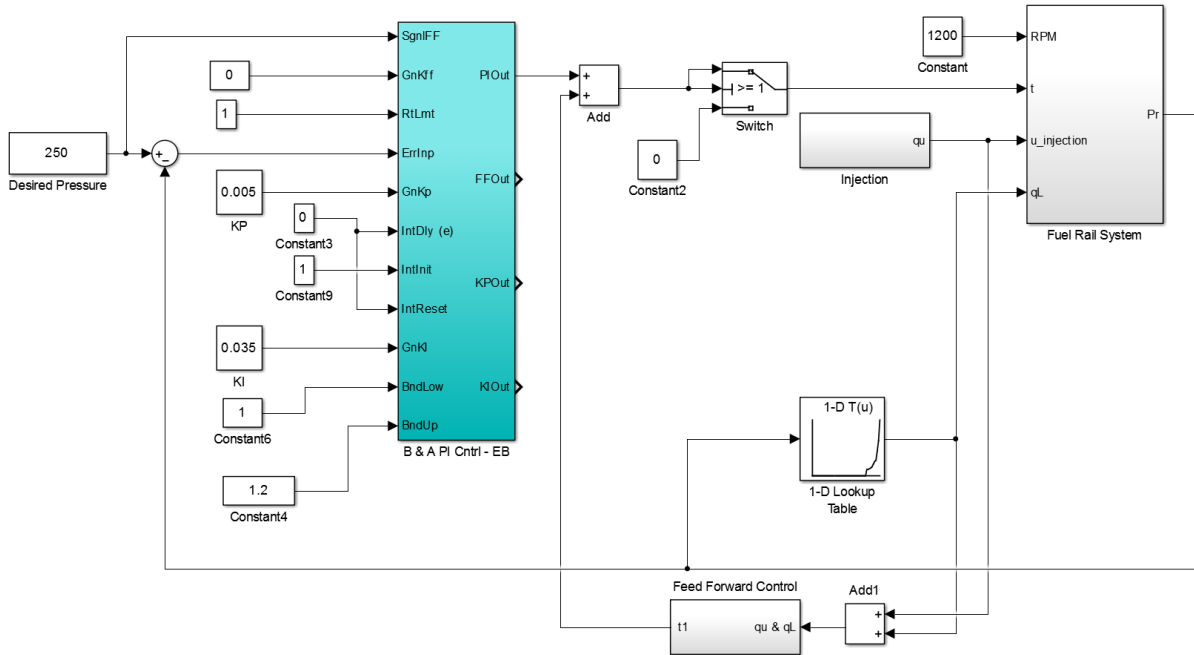
Figure 31: The Block Diagram of the Closed-loop Fuel Rail System with Controller

From the control principle, it is obvious that when the solenoid control valve is closed, the intake flow is zero. When the control valve is open, the output flow will be zero. The relationship of intake flow and output flow with a 1.2 ms control pulse is shown in Figure 32.
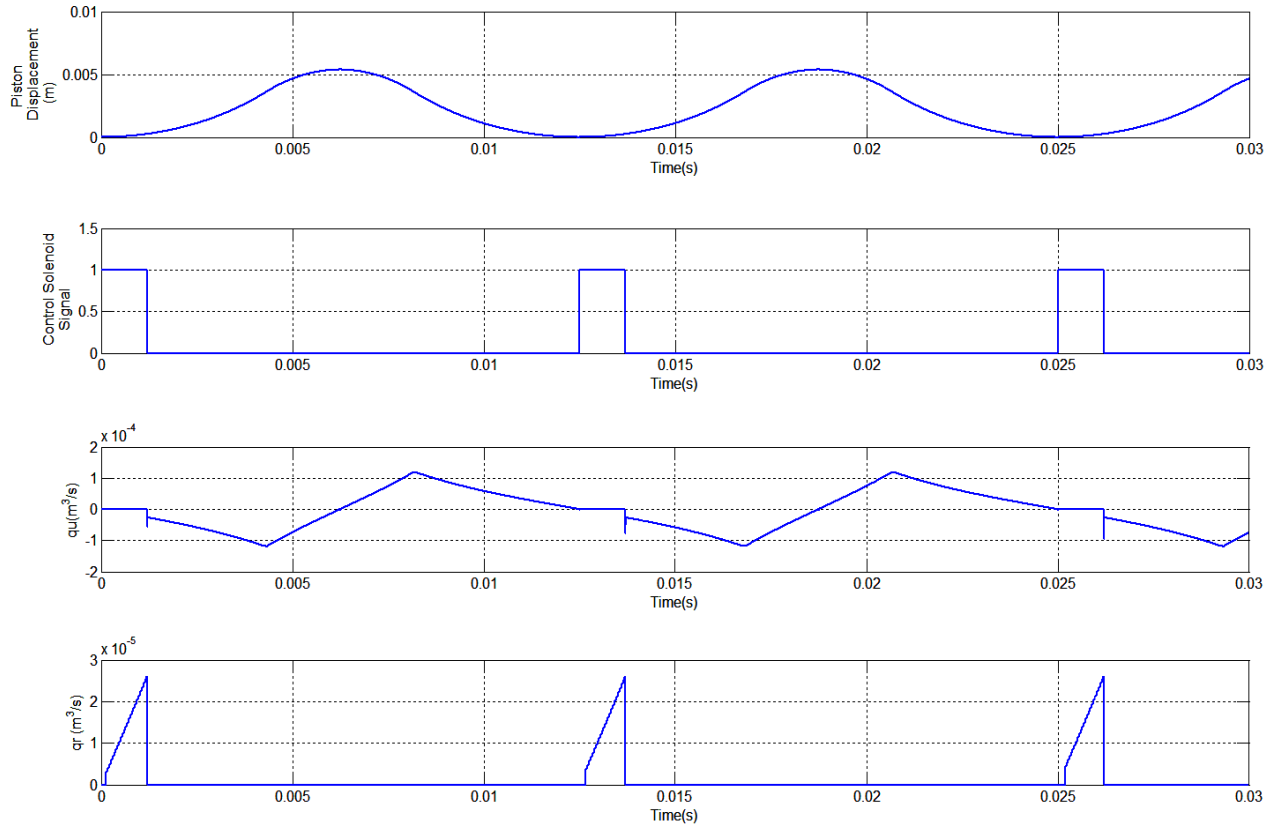
Figure 32: Relationship among Each Signal

Two different conditions are simulated using Simulink software to validate the control law. The first is the pressure tracking without fuel injection; and the second is the pressure tracking with fuel injection.

3.2.1 Tracking Validation

In this part, two desired pressures 200 bar and 250 bar, are used to validate the model and the developed controller. In the bumpless and anti-windup PI controller, the "P" gain is 0.005 and "I" gain is 0.035. The simulation result with 200 bar desired fuel pressure is shown in Figure 33. It takes about 3 seconds to reach 200 bar and the peak error is within 1%.
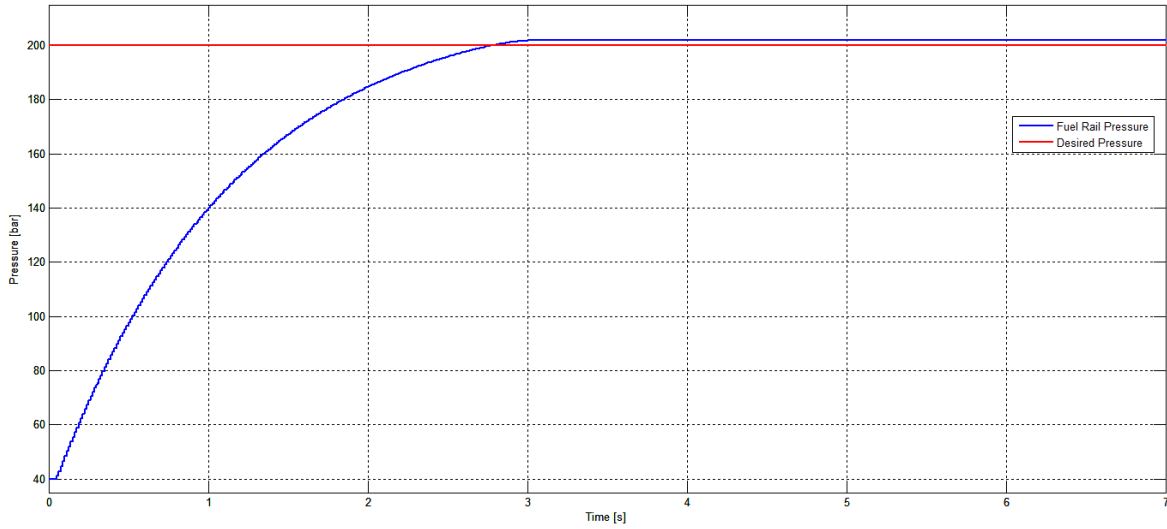
Figure 33: Simulation Result with the Desired Pressure of 200bar.

The simulation result for the case of 250 bar desired pressure is shown in Figure 34. Within 3.5s, the pressure reaches 250 bar with a max error of 0.6%.
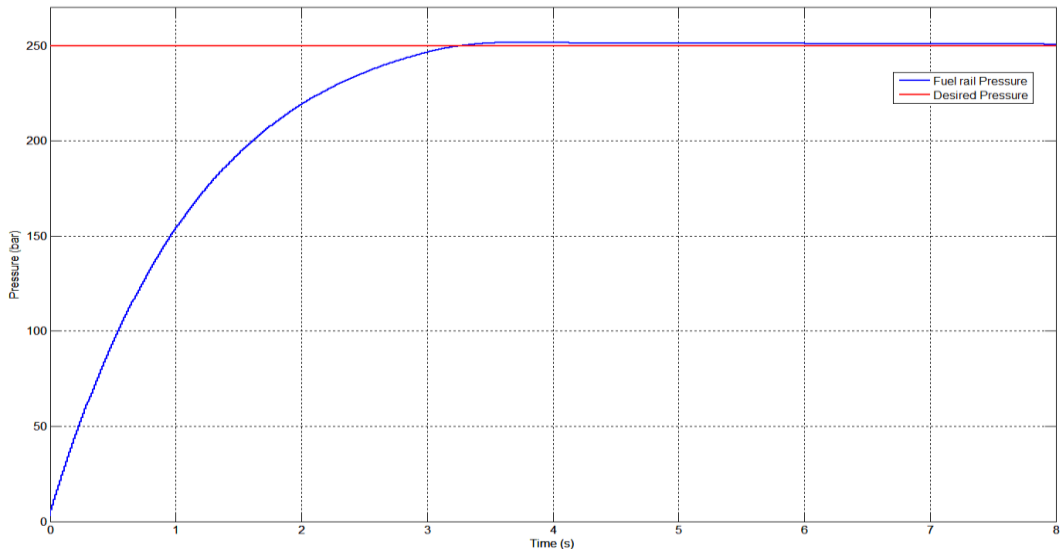

Figure 34: Simulation Result with the Desired Pressure of 250bar

37

3.2.2 Fuel Inject Flow Compensation

In the Simulink simulation, a fuel injection signal is added to study the performance of the feed-forward controller. The injection pulse width is 1.0 ms at the engine speed of 1200 RPM. When the desired fuel pressure is 200 bar without the feed-forward control, the fuel rail pressure drops to 170 bar as shown in Figure 35.
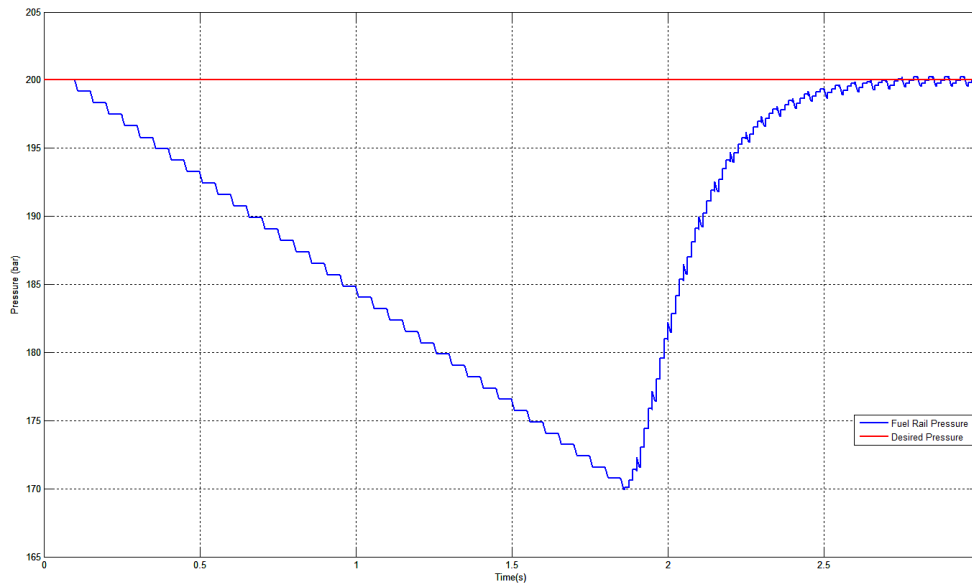

Figure 35: Injection without Feed-forward Controller at 200bar

From the simulation result shown in Figure 35, it is obvious that without the feed-forward controller, when the fuel injection starts the fuel rail pressure drops significantly. That could lead to inaccurate fuel injection under the transient engine operational conditions. The fuel rail pressure regulation under transient fuel injection with the feed-forward controller is shown in Figure 36. The fuel rail pressure error is less than 0.05%.
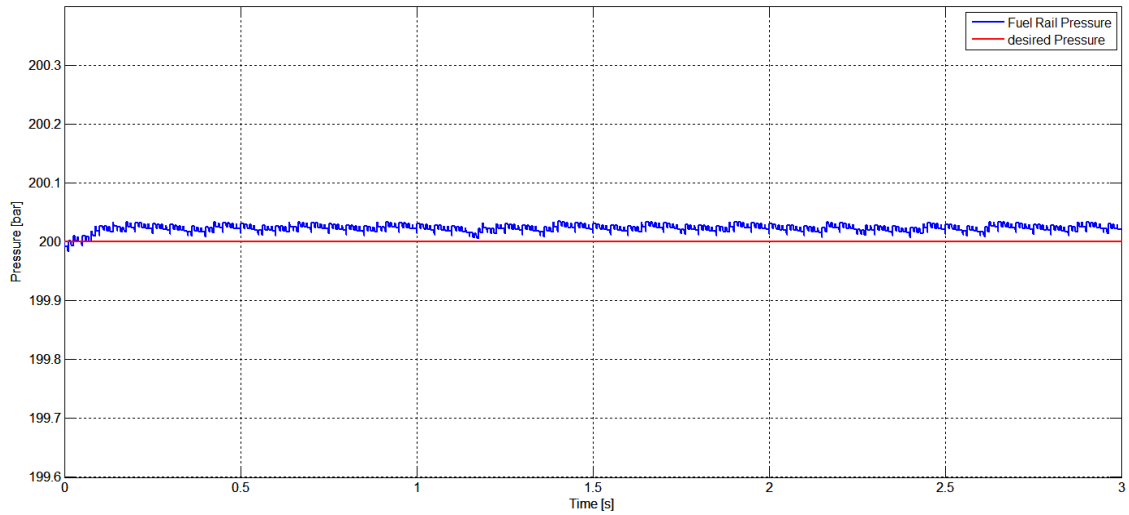
Figure 36: The Pressure Performance of the System with Feed-forward Control with Injection

       at 200bar

The fuel rail pressure under the fuel injection perturbation with the feed-forward controller at 250 bar is shown in Figure 37, where fuel rail pressure error is less than 0.05%.
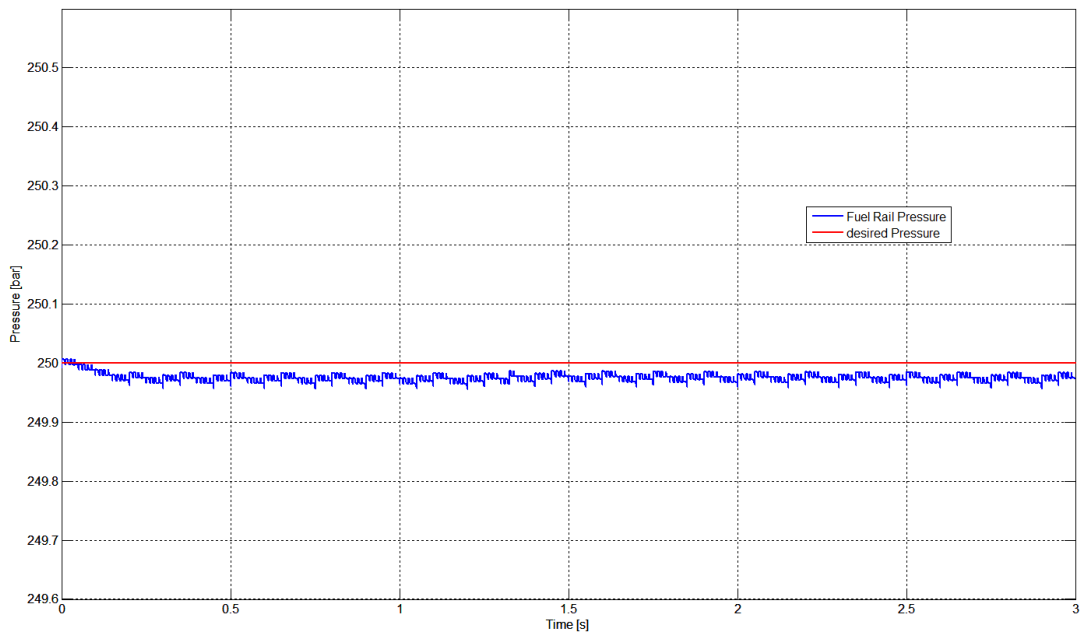

Figure 37: The Pressure Performance of the System with Feed-forward Control with Injection

       at 250bar

CHAPTER 4: EXPERIMENTAL VALIDATION

4.1 Introduction

Although the simulation model is able to demonstrate the characteristics of the fuel rail systems, it will never imitate the exact real-world system. It is necessary to validate the whole system experimentally.

In this Chapter, the fuel rail system is validated without fuel injection perturbation. In the meantime, the Simulink simulation results are compared with the experiment data.

4.2 Tracking Validation

The controller parameters used in the experiments are the same as those used in the simulations. Without fuel injection, the comparison of the experimental and simulation results are shown in Figure 38 and Figure 39.

Figure 38 shows the comparison when the desired fuel rail pressure is 200 bar. Within 3 seconds, the fuel rail pressure reaches 200 bar with a steady-state error of 0.9%.
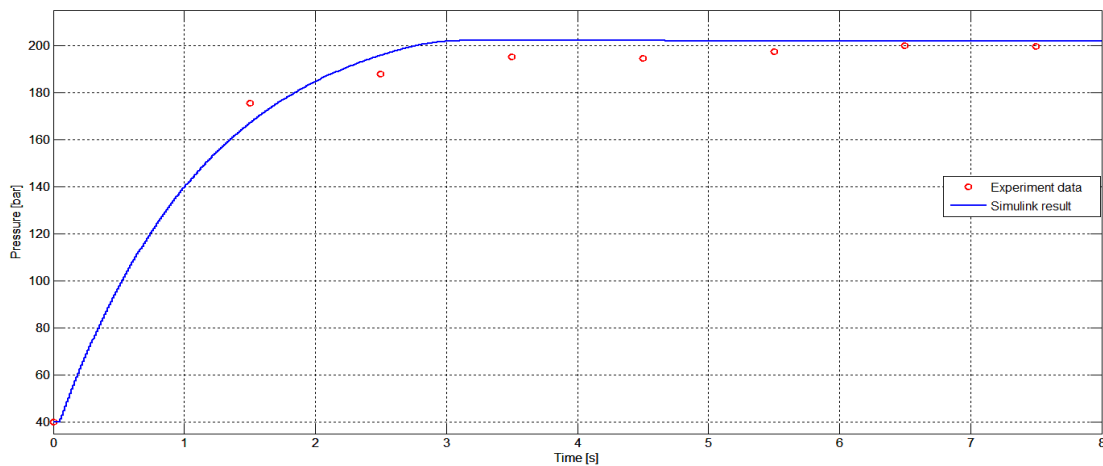

Figure 38: Comparison of the Experiment Result and Simulink Result at 200bar

Figure 39 shows the case of 250 bar desired fuel rail pressure. Within 5 seconds, the fuel rail pressure reaches 250 bar with a max steady state-error of 0.8%. The error between the simulation result (blue line) and the experiment data (red dot) is less than 2.5% at the steady state.
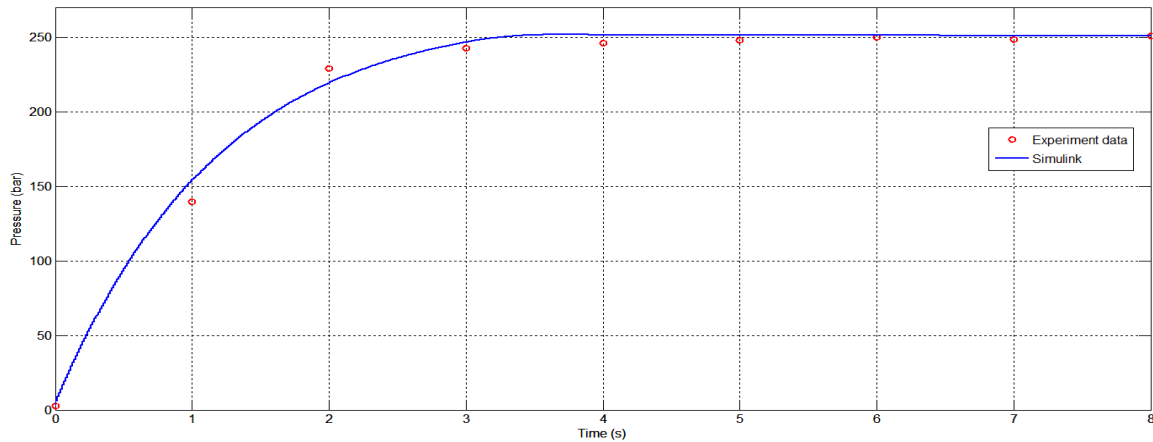

Figure 39: Comparison of the Experiment Result and Simulink Result at 250bar

4.3 Leakage Protection

Since the pressure relief valve of the fuel rail system causes certain fuel leakage near the fuel pressure of 250 bar, the fuel rail pressure varies due to the leakage flow. However, with the help of the closed-loop control, the pressure is maintained at the desired pressure. Figure 40 shows the fuel rail pressure trace when the desired fuel pressure is 250 bar. The maximum rail pressure is 252.3 bar, and the minimum is 248.2 bar, which leads to a steady-state error of less than 1%.
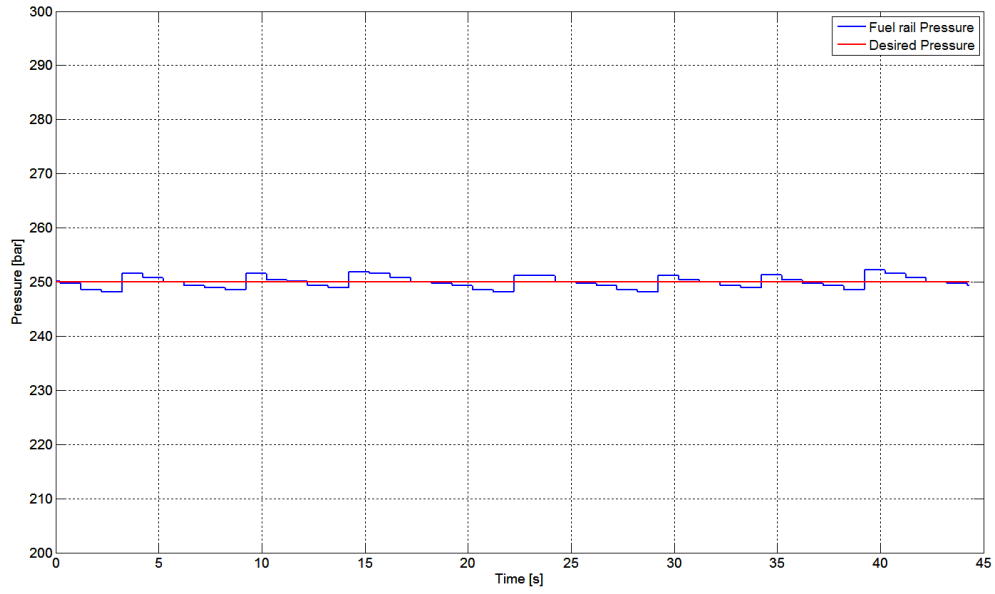
Figure 40: Leak Protection at the Desired Pressure at 250bar

CHAPTER 5: CONCLUSIONS AND FUTURE WORK

5.1 Conclusions

In this thesis, a fuel rail control system is developed. The whole system is developed based upon a MotoTron engine control module (ECM). LabVIEW GUI is used as the user graphic interface. The control system is calibrated using the MotoTune software. The MotoTron ECM communicates with the MotoTune and LabVIEW GUI through its CAN links.

To meet the fuel rail pressure control requirements of a GDI engine fuel system, in this thesis, a control-oriented mathematical model of a fuel rail system for a GDI engine is developed using MATLAB/Simulink. The Simulink model is then used to develop and validate the pressure control strategy before the pressure controller is validated experimentally. By comparing the experiment data, the simulation results show that the mathematical model is able to replicate the behavior of the actual fuel rail system.

The pressure control strategy of the fuel rail system consists of three parts: a bumpless and anti-windup PI Controller, a feed-forward controller, and a dead-zone compensator. By validating the pressure controller both in simulations and experiments, the control strategy is validated. And the closed-loop controller is able to meet the fuel pressure regulation requirements.

5.2 Future Recommendations

In this thesis, the fuel rail system is able to maintain the fuel rail pressure at the desired pressure with or without the fuel injection perturbation. However, the fuel system efficiency and performance is not considered and it could be improved through further calibrations of the start

position of solenoid control pulse or decreasing the number of pulses. The fuel rail control system can be further improved by using advanced control strategies.

For the effect of fuel injection, it is important to validate it experimentally and additional control calibrations would be required.

APPENDICES

APPENDIX A – Fuel Pump Harness
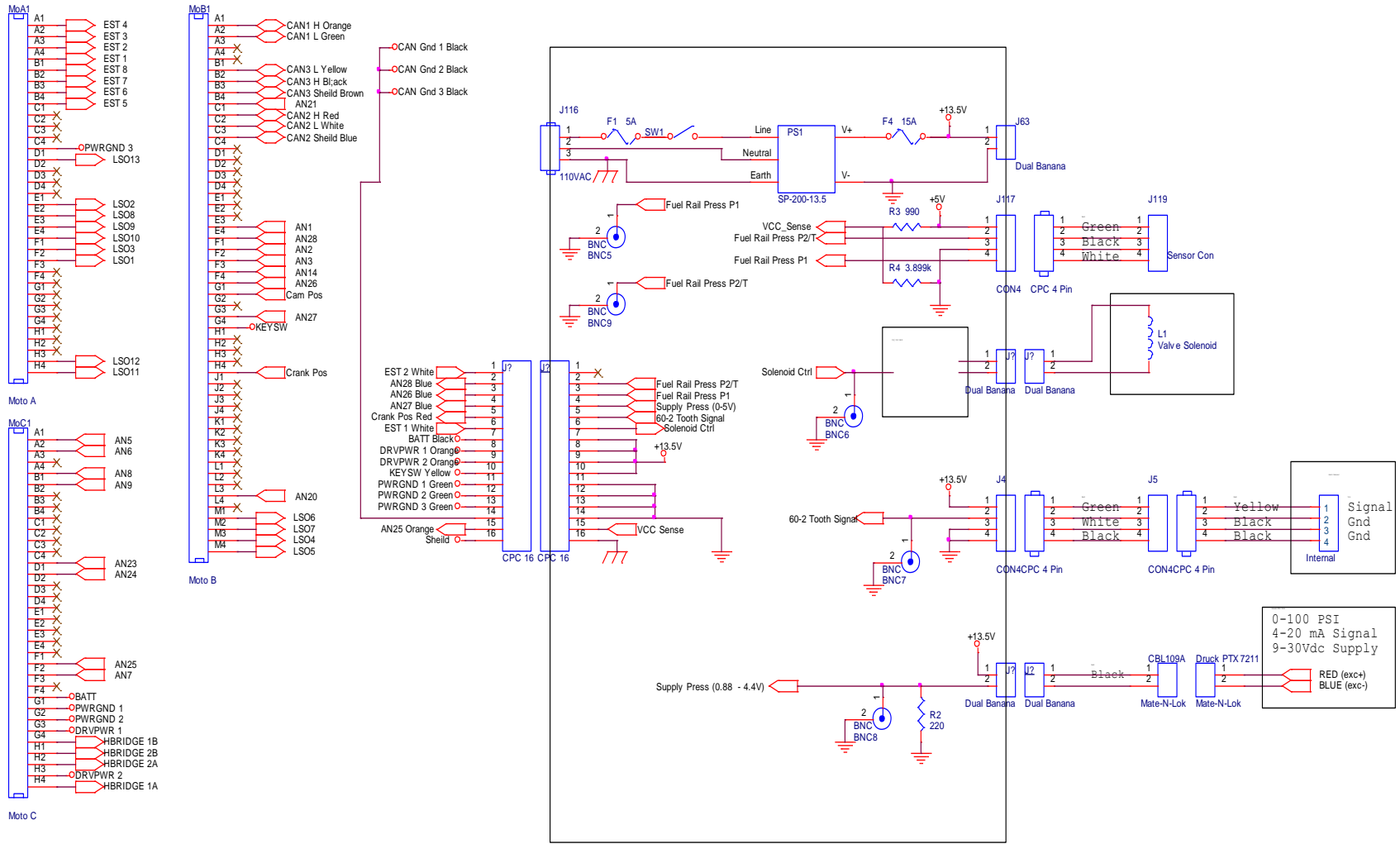
Figure 41: Fuel Pump Harness

APPENDIX B – MotoTron Simulink Diagram
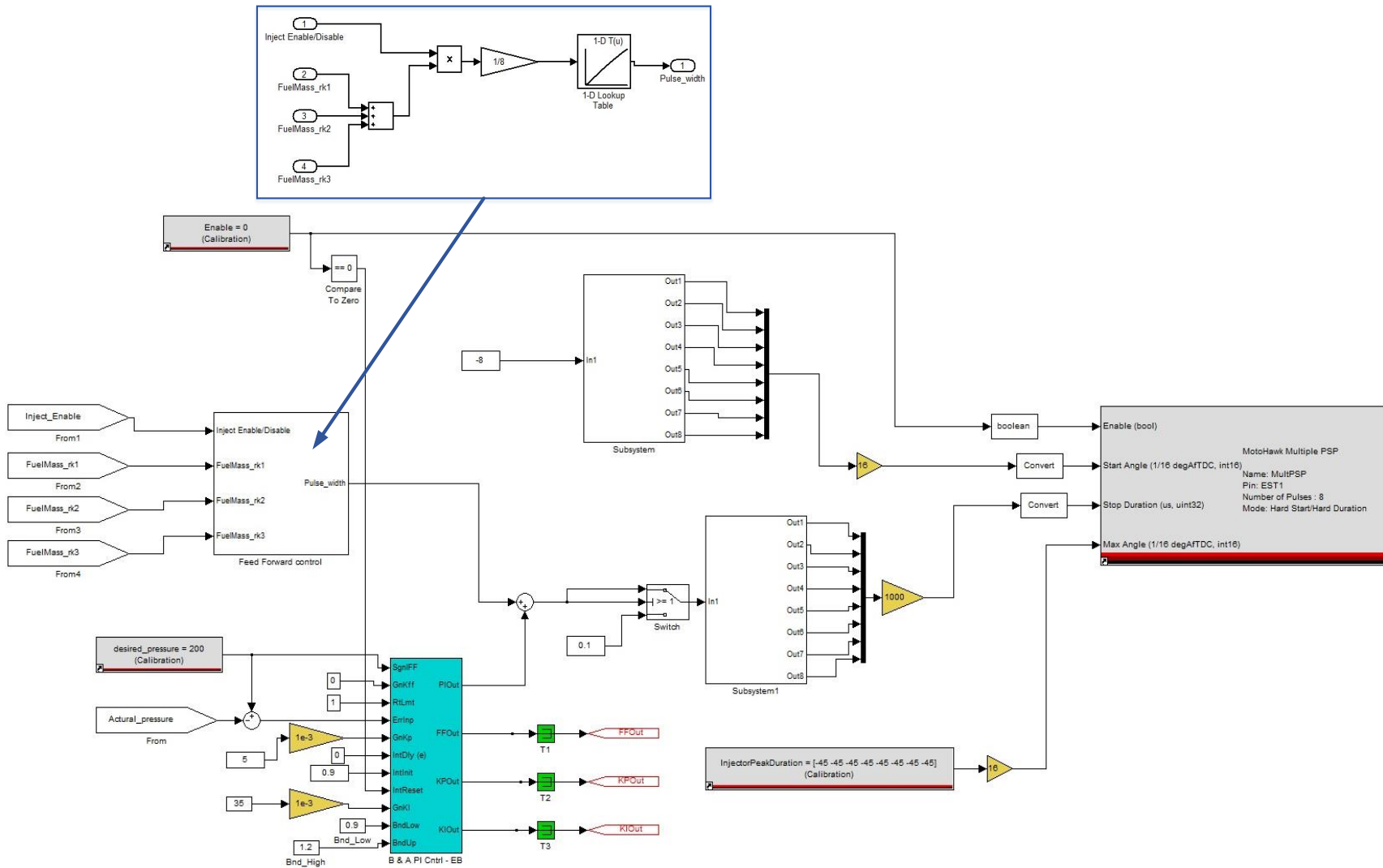
Figure 42: MotoTron Simulink Diagram

REFERENCES

REFERENCES

[1] U. Spicher, J. Reissing, J. M. Kech and J. Gindele "Gasoline Direct Injection (GDI) Engines-Development Potentialities," *SAE International*, 1999 (doi: 10.4271/1999-01-2938).

[2] Autuan Goodwin "What's so Great about Direct Injection," *ABCs of Car Tech*

[3] R. Morselli, E. Corti and G. Rizzoni, "Energy Based Model of a Common Rail Injector," *Proc. Of the 2002 IEEE Int. Conf. on Control App, Glasgow, Scotland, September 2002*, pp. 1195-1200

[4] P. Lino, B. Maione, and A Rizzo, "Nonlinear Modeling and Control on a Common Rail Injection System for Diesel Engines," *Applied Mathematical Modelling*, Vol.31, 1959, pp. 1770-1784.

[5] D.A. Kouremenos, D.T. Hountalas, A.D. Kouremenos, "Development and Validation of a Detailed Fuel Injection System Simulation Model for Diesel Engines," *SAE Technical Paper*, 1999 (doi: 10.4271/1999-01-0527).

[6] Pengyuan Sun, Baiyu Xin, H Chen and J. Li, "Model Based Nonlinear Controller Design for Fuel Rail System of GDI Engine," *Proceedings of the FISITA 2012 World Automotive Congress Lecture Notes in Electrical Engineering ,2013*, pp 503-514

[7] Umberto Montanaro, Alessandro di Gaeta, Veniero Giglio, "An MARC Approach for Tracking and Ripple Attenuation of the Common Tail Pressure for GDI Engines," *18th IFAC World Congress Milano (Italy) 2011*, (doi: 10.3182/20110828-6-IT1002.02843)

[8] Tom Boynton, "General Motors Computerized Vehicle Control System: A short History", CET249,2006

[9] MotoHawk MotoTune Software Calibration Development Tool, *Product Specification 37748, 2015*

[10] Gasoline Direct Injection Key Technology for Greater Efficiency and Dynamics, BOCSH

[11] V. Streeter, K. Wylie, E. Bedford, "Fluid Mechanics, Ninth Ed.", New York 1998

[12] D. T. Hountalas, A. D. Kouremenos, "Development of a Fast and Simple Simulation Model for the Fuel Injection System of Diesel Engines", *Adv. Eng. Software 29 (1) (1988) 13-28*

[13] Sam Mannan, Frank P. Lee, "Lees' Loss Prevention in the Process Industries：Hazard Identification, Assessment and Control", ISBN: 0-7506-7857-7

[14] George Zhu G, Mark W. Pyclik, Eric K Bradley, Larry J. Brackney, "Close-loop Actuator control system Having Bumpless Gain and Anti-windup Logic" *IPC F02D 35/00 (2006.01), F02D 41/14 (2006.01), F02D 43/00 (2006.01)*

[15] Jerry Banks; John S. Carson; Barry L. Nelson; David M. Nicol, "Discrete-Event System Simulation Fifth Edition" *Upper Saddle River, Pearson Education, Inc. 2010* ISBN 0136062121

[16] Abu-Taieh, Evon M. O. "Handbook of Research on Discrete Event Simulation Environments: Technologies and Applications"